

Dynamic Jump Intensities and Risk Premiums in Crude Oil Futures and Options Markets

Peter Christoffersen

University of Toronto, CBS, and CREATES

Kris Jacobs

University of Houston and Tilburg University

Bingxin Li

University of Houston

October 17, 2012

Work in Progress

Please do not cite

Abstract

Options on crude oil futures are the most actively traded commodity derivatives. Existing pricing models for crude oil derivatives are computationally intensive due to the presence of latent state variables. We adopt a class of computationally efficient discrete-time jump models that allow for closed-form option valuation, and investigate the economic importance of jumps and dynamic jump intensities in the market for crude oil futures and futures options. Including jumps is crucial for modeling crude oil futures and futures options, and we find very strong evidence in favor of time-varying jump intensities. The main role of jumps and jump risk in the crude oil futures and options markets is to capture excess kurtosis in the data. We find that jumps account for a large part of the variation in crude oil futures and options prices, and a substantial part of the risk premium is due to jumps. Futures data indicate the presence of many small jumps, while option data point towards large infrequent jumps.

JEL Classification: G12; G13.

Keywords: Crude oil; Futures; Options; Discrete-time models; Jump intensities; Risk premiums.

1 Introduction

Crude oil is the single largest commodity in international trade, and the crude oil derivatives market constitutes the most liquid commodity derivatives market. In December 2011, WTI and Brent crude oil futures accounted for 51.4% of dollar weight in the S&P GSCI commodity index. Nearly 900,000 futures and options contracts trade on WTI every day.

In order to price and hedge this increasingly important commodity, it is crucial to model crude oil futures and options and better understand their dynamics. Surprisingly though, there are relatively few studies on pricing crude oil derivatives, especially when compared with the existing literature on equity derivatives. Trolle and Schwartz (2009) estimate a continuous-time stochastic volatility model using NYMEX crude oil futures and options and find evidence for two, predominantly unspanned, volatility factors. They do not consider jump processes, which have been used in other security markets to model large movements. Larsson and Nossman (2010) examine the performance of affine jump diffusion models with stochastic volatility for modeling the time series of crude oil spot prices. Their results show that stochastic volatility alone is not sufficient and jumps are an essential factor to correctly capture the time series properties of oil prices. However, they do not use panel data on futures contracts nor option prices. Hamilton and Wu (2011) model crude oil futures with an affine term structure model and document significant changes in oil futures risk premia since 2005. Pan (2011) studies the relationship of state price densities and investor beliefs. Chiarella, Kang, Sklibosios, and To (2012) document a hump-shaped volatility structure in the commodity derivatives market. To the best of our knowledge, no existing studies have implemented jump models using extensive cross-sections of crude oil derivatives.

There is an extensive literature on the modeling of equity derivatives, which mainly focuses on index returns and options. This literature includes models with both stochastic volatility and jumps (e.g., see Bakshi, Cao, and Chen, 1997; Bates, 1996, 2000, 2006; Pan 2002; Eraker, 2004; Carr and Wu, 2004; Santa-Clara and Yan 2010,), as well as GARCH-style jump models (Maheu and McCurdy, 2004; Duan, Ritchken and Sun, 2006, Christoffersen, Jacobs, and Ornathanalai, 2012; and Ornathanalai, 2012).

The implementation of continuous-time stochastic volatility models with Poisson jumps is complex, because the likelihood function is typically not available in closed form, and therefore option pricing in the presence of jumps typically relies on complex econometric methods to filter the unobserved state variables. For example, Chernov, Gallant, Ghysels, and Tauchen (2003) use an Efficient Method of

Moments (EMM) based method, Pan (2002) uses the implied-state Generalized Method of Moments (GMM) technique, Eraker, Johannes, and Polson (2003), Eraker (2004), and Li, Wells, and Yu (2007) employ Markov Chain Monte Carlo (MCMC) techniques, and Trolle and Schwartz (2009) use the Extended Kalman Filter (EKF). This type of estimation is computationally intensive, especially when dealing with large data sets.

In this paper, we study discrete-time models in which the conditional variance of the normal innovation and the conditional jump intensity of a compound Poisson process are governed by GARCH-type dynamics. We estimate four nested jumps models to investigate the importance of time-varying conditional variance and time-varying jump intensity using an extensive panel data set of crude oil futures and option prices.

For the discrete-time models in this paper, both the conditional jump intensity and the conditional variance can be directly computed from the observed shocks using an analytical filter. With the analytical filter, filtering the normal component and the jump component is relatively simple and extremely fast, even when the jump intensity is time-varying. It takes less than a second to filter 38,024 futures contracts using Matlab on a standard PC. Because the variance and the jump intensity dynamic can be updated analytically, we can conveniently estimate the model using MLE or NLS estimation. Calculating the Implied Volatility Root Mean Squared Error (IVRMSE) of 283,653 option contracts takes about 7 seconds.

We investigate the economic importance of jumps and dynamic jump intensity in the crude oil market and compare the fit of the jump models with that of a benchmark GARCH model without jumps. We study four jump models with different specifications of jump intensity and conditional variance. The DVCJ (dynamic volatility with constant jumps) model is assumed to have constant jump intensities, which is consistent with most of the existing continuous-time SVJ literature. The CVDJ (constant volatility and dynamic jumps) model has time-varying jump intensity, but the normal innovation to the return process is assumed to be homoskedastic. It is related to the constant volatility jump-diffusion models of Bates (1991) and Merton (1976). The DVDJ (dynamic volatility and dynamic jumps) model contains time-varying jump intensities and a time-varying conditional variance but the dynamics are driven by the same dynamic. The DVSDJ (dynamic volatility with separate dynamic jumps) model is the most general model in which both the jump intensity and the conditional variance are time-varying and the dynamics are modeled separately. The latter two models are related to the most complex SVJ dynamics of Eraker (2004) and Santa-Clara and Yan (2010).

We find strong evidence of the presence of jumps and dynamic jump intensities in the crude oil market. During crisis periods, when market risk is high, jumps occur more frequently. Jump models with time-varying jump intensities outperform the benchmark model significantly, and in models with time-varying intensities jumps explain a large part of the variance of the underlying futures data, regardless of the data used in estimation.

Estimates based on futures data indicate the presence of many small jumps, whereas estimates based on option data point towards infrequent large jumps. The implied conditional kurtosis from option-based estimates is much larger than that implied by futures data. Contrary to equity index markets, the main role of jumps and jump risk in crude oil futures markets is to capture the excess kurtosis in the data, while skewness is of second-order importance.

The rest of the paper proceeds as follows. Section 2 develops discrete-time pricing models for commodity futures. We propose four nested jump models and a benchmark GARCH model. Section 3 discusses the crude oil futures and options data used in this paper. In Section 4 we explain MLE estimation on futures contracts and report the estimation results. Section 5 derives the risk-neutral dynamics and the closed form option valuation formula. Section 6 presents estimation results using options data, and Section 7 presents results using options and futures jointly in estimation. Section 8 concludes.

2 Models for Commodity Futures Markets

In commodity futures markets, we observe futures prices for different maturities, and spot prices are considered unobservable. We develop a general class of discrete-time models by first specifying models for the unobservable spot price, and then imposing the relationship between the spot price and futures prices for different maturities.

The relationship between the futures price and the spot price of a commodity is given by

$$F(t, T) = S(t) \exp [c(t, T) * (T - t)] \quad (2.1)$$

where $S(t)$ denotes the spot price at time t , $F(t, T)$ is the time t price of the futures contract maturing at time T , and $c(t, T)$ denotes the time t forward cost of carry for the futures contract maturing at T . Combining this with the expression for the time $t+1$ futures price maturing at time T , the log futures return is given by

$$\log \frac{F_{t+1,T}}{F_{t,T}} = \log \frac{S_{t+1}}{S_t} + \Delta c(t, t+1, T) \quad (2.2)$$

where $\Delta c(t, t+1, T)$ captures the cumulative difference of the forward cost of carry between time t and $t+1$ for futures contracts maturing at time T .

The forward cost of carry $c(t, T)$ is unobservable. We assume it is deterministic, and extract it from the relationship between futures and spots prices following the approach of Gibson and Schwartz (1990). We provide details on this method in Appendix A. Several studies have estimated more general models with stochastic cost of carry specifications. We implemented stochastic cost of carry models, but for the models under study here the cost of carry model does not seem to substantially affect the results.

2.1 The Benchmark Model

We formulate a new class of jump models for commodities markets. To provide a benchmark for these models that can capture several important stylized facts of commodity markets, we first consider a standard GARCH model. We specify the spot return process

$$\log \frac{S_{t+1}}{S_t} = r_{t+1} + \left(\lambda_z - \frac{1}{2} \right) h_{z,t+1} + z_{t+1} \quad (2.3)$$

Where r_{t+1} is the instantaneous risk free rate, z_{t+1} is an innovation which is distributed $N(0, h_{z,t+1})$, $h_{z,t+1}$ is the conditional variance known at time t , and λ_z is the market price of risk associated with the normal innovation.

Substituting (2.3) into (2.2), we get the benchmark GARCH model for futures returns

$$\log \frac{F_{t+1,T}}{F_{t,T}} = r_{t+1} + \left(\lambda_z - \frac{1}{2} \right) h_{z,t+1} + \sqrt{h_{z,t+1}} \varepsilon_{z,t+1} + \Delta c(t, t+1, T) \quad (2.4)$$

where $\varepsilon_{z,t+1}$ is distributed $N(0,1)$. The conditional variance of the normal innovation $h_{z,t+1}$ is governed by a GARCH (1, 1) process, which is specified according to Heston and Nandi (2000).

$$h_{z,t+1} = \omega_z + b_z h_{z,t} + a_z (\varepsilon_{z,t} - c_z \sqrt{h_t})^2 \quad (2.5)$$

GARCH models provide a convenient framework to capture stylized facts in financial markets such as conditional heteroskedasticity, volatility clustering, and mean reversion in volatility. These stylized facts are also very prominent in commodity futures markets. The GARCH dynamic in (2.5) is different from the more conventional GARCH specifications of Engle (1982) and Bollerslev (1986), and is explicitly

designed to facilitate option valuation. We discuss the benefits of the specification in (2.5) in more detail below.

Consistent with other GARCH specifications, the conditional variance $h_{z,t+1}$ in (2.5) is predictable conditional on information available at time t . The unconditional variance is given by $E[h_{z,t+1}] = (\omega_z + a_z)/(1 - b_z - a_z c_z^2)$, where $b_z + a_z c_z^2$ is the variance persistence. Further, given a positive estimate for a_z , the sign of c_z determines the correlation between the futures returns and the conditional variance. Equivalently, c_z can be thought of as controlling the skewness or asymmetry of the distribution of log returns, with a positive c_z resulting in a negatively skewed multi-day distribution.

2.2 Filtering the Conditional Variance Using Futures with Different Maturities

Heston and Nandi (2000) estimate their model using S&P 500 index returns and options. For that application, it is straightforward to directly filter the conditional variance $h_{z,t+1}$ from the return innovations with the GARCH model. Our application is more complex, because we have a cross-section of crude oil futures prices with different maturities (eight time series of futures contracts in our case).

Consider the following futures return series

$$\log \frac{F_{t+1, T_i}}{F_{t, T_i}} = r_{t+1} + \left(\lambda_{i,z} - \frac{1}{2} \right) h_{i,z,t+1} + \sqrt{h_{i,z,t+1}} \varepsilon_{i,z,t+1} + \Delta c(t, t+1, T_i) \quad (2.6)$$

where $i = 1, 2, \dots, 8$ and T_i represents the maturity date of the futures contract. The number of parameters in this model is very large if the parameters for the return and variance dynamics are maturity-specific, and the number of parameters increases with the number of futures contracts. Instead, impose the restriction that these parameters are the same for all eight maturities. Furthermore, instead of separate dynamics for each maturity, consider filtering the volatility using

$$\begin{aligned} h_{z,t+1} = & \omega_z + b_z h_{z,t} + a_z (\varepsilon_{1,z,t} - c_z \sqrt{h_{z,t}})^2 + a_z (\varepsilon_{2,z,t} - c_z \sqrt{h_{z,t}})^2 + \dots \\ & + a_z (\varepsilon_{8,z,t} - c_z \sqrt{h_{z,t}})^2 \end{aligned} \quad (2.7)$$

Finally, we have to specify the structure of the covariance matrix of the vector of residuals. To keep the model as parsimonious as possible and further reduce the number of parameters, we assume that covariance matrix of the return innovations is a diagonal matrix, $\varepsilon_{z,t+1} = [\varepsilon_{1,z,t+1}, \varepsilon_{2,z,t+1}, \dots,$

$\varepsilon_{8,z,t+1}] \sim \text{i.i.d. } N(0, I_8)$, where I_8 is the identity matrix. This approach is consistent with the assumptions made by Trolle and Schwartz (2009), who use the Kalman filter for estimation.

2.3 Commodity Futures Returns with Dynamic Jump Intensities

The futures return process in (2.4)-(2.5) provides a benchmark model that can capture several important stylized facts using a simple setup with a single normal innovation. We now provide a much richer class of models with jumps in returns and volatilities, and with potentially time-varying jump intensities. Futures returns are given by

$$\log \frac{F_{t+1,T}}{F_{t,T}} = r_{t+1} + \left(\lambda_z - \frac{1}{2} \right) h_{z,t+1} + (\lambda_y - \xi) h_{y,t+1} + z_{t+1} + y_{t+1} + \Delta c(t, t+1, T). \quad (2.8)$$

where the notation for r_{t+1} , λ_z , z_{t+1} and $h_{z,t+1}$ is the same as in Section 2.1. The jump component y_{t+1} is specified as a Compound Poisson process denoted as $J(h_{y,t+1}, \theta, \delta^2)$. The Compound Poisson structure assumes that the jump size is independently drawn from a normal distribution with mean θ and variance δ^2 . The number of jumps n_{t+1} arriving between times t and $t+1$ is a Poisson counting process with intensity $h_{y,t+1}$. The jump component in period $t+1$ is therefore given by

$$y_{t+1} = \sum_{j=0}^{n_{t+1}} x_{t+1}^j \quad (2.9)$$

where $x_{t+1}^j, j = 0, 1, 2, \dots$ is an *i.i.d.* sequence of normally distributed random variables, $x_{t+1}^j \sim N(\theta, \delta^2)$. The conditional expectation of the number of jumps arriving over time interval $(t, t+1)$ equals the jump intensity, $E_t[n_{t+1}] = h_{y,t+1}$. The conditional mean and variance of the jump component y_{t+1} are given by $\theta h_{y,t+1}$ and $(\theta^2 + \delta^2) h_{y,t+1}$ respectively.

The convexity adjustment terms $\frac{1}{2} h_{z,t+1}$ and $\xi h_{y,t+1} \equiv (e^{\theta + \frac{\delta^2}{2}} - 1) h_{y,t+1}$ in (2.6) act as compensators to the normal and jump component respectively. The conditional risk premium is given by $\gamma_{t+1} \equiv \lambda_z h_{z,t+1} + \lambda_y h_{y,t+1}$, with λ_z and λ_y denoting the market prices of risks for the normal and jump components.

2.4 Four Jump Models

We formulate four nested models with jump dynamics. In the most general model, we assume that both the conditional variance of the normal component and the jump intensity are governed by the following extended GARCH (1, 1) dynamics.

$$h_{z,t+1} = \omega_z + b_z h_{z,t} + \frac{a_z}{h_{z,t}} (z_t - c_z h_{z,t})^2 + d_z y_t \quad (2.10)$$

$$h_{y,t+1} = \omega_y + b_y h_{y,t} + \frac{a_y}{h_{z,t}} (z_t - c_y h_{z,t})^2 + d_y y_t \quad (2.11)$$

where $\omega_z, a_z, b_z, c_z, d_z, \omega_y, a_y, b_y, c_y, d_y$ are parameters to be estimated.

We refer to this specification as the Dynamic Volatility and Separate Dynamic Jumps (DVSDJ) model. It is a very rich and flexible model. First, it allows for jumps in volatility as well as jumps in returns. It has been shown in the index option literature that jumps in volatility are useful to explain option volatility smiles and smirks (see for example Eraker, Johannes and Polson, 2003; and Eraker, 2004). Moreover, in (2.10)-(2.11), the normal and jump innovations, z_t and y_t , enter separately into the GARCH updating dynamics. The model therefore allows each type of innovation to impact the variance and jump intensity separately. Second, the model is designed to yield closed-form expressions for securities prices. Critically, we are able to derive analytical results for option valuation.

The specification of $h_{z,t+1}$ and $h_{y,t+1}$ in (2.10)-(2.11) therefore has substantial advantages. One potential problem is that the model is richly parameterized. This presumably will not create problems for in-sample option valuation, but it may cause the model's out-of-sample performance to deteriorate. We therefore also investigate three nested specifications, which impose restrictions on $h_{z,t+1}$ and $h_{y,t+1}$, and greatly reduce the dimension of the parameter space.

The first nested model is the Dynamic Volatility and Constant Jumps (DVCJ) model, which imposes the following restrictions

$$b_y = 0, \quad a_y = 0, \quad c_y = 0, \quad d_y = 0 \quad (2.12)$$

This model maintains the normal component's GARCH dynamic, but jumps arrive at a constant rate ω_y , regardless of the level of volatility in the market.

The second nested model is the Constant Volatility and Dynamic Jumps (CVDJ) model, which imposes the restrictions

$$b_z = 0, \quad a_z = 0, \quad c_z = 0, \quad d_z = 0 \quad (2.13)$$

In this model, time-variation in the return distribution is driven by the jump component only. The normal component of returns is homoskedastic, with a constant variance equal to ω_z .

In the third nested model, the Dynamic Volatility and Dynamic Jumps (DVDJ) model, $h_{z,t+1}$ and $h_{y,t+1}$ are both time-varying but driven by the same dynamic. The conditional jump intensity is affine in the conditional variance of the normal component

$$h_{y,t+1} = kh_{z,t+1} \quad (2.14)$$

where k is a parameter to be estimated. The DVDJ specification can be written as a special case of the DVSDJ model, subject to the following restrictions on the parameters of $h_{y,t+1}$

$$\omega_y = \omega_z k, \quad b_y = b_z, \quad a_y = a_z k, \quad c_y = c_z, \quad d_y = d_z k \quad (2.15)$$

The specification of these four models is based on the index returns models in Ornathanalai (2012) and Christoffersen, Jacobs, and Ornathanalai (CJO, 2012). We follow the classification of jump models proposed in CJO (2012), but the model dynamics in (2.10)-(2.11) are different in a very important way. They are designed to yield a closed-form solution for option prices, and in order to do so we have adopted a rather simple specification for jumps in volatility. The drawback of this approach is that we cannot ensure positive volatility.

3. Crude Oil Futures and Options Data

We now discuss the crude oil futures and options data used in the empirical analysis, and present summary statistics.

We use a data set of Chicago Mercantile Exchange (CME group, formerly NYMEX) crude oil futures and options data. We use a sample of daily data from January 2nd, 1990 to December 3rd, 2008. The CME crude oil derivatives market is the world's largest and most liquid commodity derivatives market. The range of maturities covered by futures and options and the range of option strike prices are also greater than for other commodities (for a discussion see Trolle and Schwartz, 2009, henceforth TS).

We screen futures contracts based on patterns in trading activity. Open interest for futures contract tends to peak approximately two weeks before expiration. Among futures and options with more than two weeks to expiration, the first six monthly contracts tend to be very liquid. For contracts with maturities over six months, trading activity is concentrated in the contracts expiring in March, June, September, and December.

Following TS (2009), we therefore screen the available futures and options data according to the following procedure: discard all futures contracts with 14 or less days to expiration. Among the remaining, retain the first six monthly contracts. Furthermore, choose the first two contracts with expiration either in March, June, September or December. This procedure leaves us with eight futures contract series which we label M1, M2, M3, M4, M5, M6, Q1, and Q2.

We include the following options on these eight futures contracts. For each option maturity, we consider eleven moneyness intervals: 0.78-0.82, 0.82-0.86, 0.86-0.90, 0.90-0.94, 0.94-0.98, 0.98-1.02, 1.02-1.06, 1.06-1.10, 1.10-1.14, 1.14-1.18, and 1.18-1.22. Moneyness is defined as option strike divided by the price of the underlying futures contract. Among the options within a given moneyness interval, we select the one that is closest to the mean of the interval.

Our data consist of American options on crude oil futures contracts.¹ CME has also introduced European-style crude oil options, which are easier to analyze. However, the trading history is much shorter and liquidity is much lower than for the American options. Since the pricing formulae are designed for European options, we have to convert the American option prices to European option prices. We assume that the price of the underlying futures contract follows a geometric Brownian motion. This specification allows for very accurate pricing of the American option using the Barone-Adesi and Whaley (1987) formula. Inverting this formula yields a log-normal implied volatility, from which we can subsequently obtain the European option price using the Black (1976) formula. To minimize the effect of errors in the early exercise approximation, we use only OTM and ATM options, i.e., puts with moneyness less than one and calls with moneyness greater than one. In addition, we only consider options that have open interest in excess of 100 contracts and options with prices larger than 0.10 dollars.

This data filtering procedure yields 38,024 futures contracts and 283,653 option contracts observed over 4,753 business days. The number of futures contracts is 8 on every day of the sample, while the number of option contracts is between 23 and 87.

Figure 1 displays the prices of the futures contracts. All prices in this paper are settlement prices.² To avoid cluttering the figure, we only display the futures term structure on Wednesdays. Futures prices increase dramatically between 2003 and 2007, and subsequently decline. Consistent with existing studies (Trolle and Schwartz (2009), Litzenberger and Rabinowitz (1995)), we find that the crude oil market is on

¹ Futures contracts expire on the third business day prior to the 25th calendar day (or the business day right before it if the 25th is not a business day) of the month that precedes the delivery month. Options written on futures expire three business days prior to the expiration date of the futures.

² The CME light, sweet crude oil futures contract trades in units of 1000 barrels. Prices are quoted in US dollars per barrel.

average in backwardation. Also, the price of long maturity futures contracts such as Q2 is lower than that of short maturity futures contracts. Figure 2 plots the daily returns, $\log \frac{F_{t+1,T}}{F_{t,T}}$, for the eight (M1, M2, M3, M4, M5, M6, Q1, Q2) futures contracts and Panel A of Table 1 provides summary statistics. Table 1 indicates that futures returns on longer maturities futures contracts, e.g., Q2 futures contracts, are less volatile than futures returns for shorter maturity contracts. However, Figure 2 indicates that returns of futures contracts with long maturity seem to have more spikes, which can be interpreted as jumps.

Table 1 also reports summary statistics for higher moments of the daily futures returns. On average across maturities, skewness is -0.91 and kurtosis is 14.77. The daily crude oil futures return series is thus skewed towards the left, indicating that there are more negative than positive outlying returns in the crude oil market. Moreover, the return series is characterized by a distribution with tails that are significantly thicker than a normal distribution.

Panel B of Table 1 lists the average number of option contracts across maturity and moneyness. The number of option contracts decreases with maturity. Among the 11 moneyness intervals, the number of option contracts is highest in the ATM interval. Panel C reports the average option prices. As expected, the average price of the option contracts increases as the maturity of underlying futures contracts increases.

Figure 3 displays the implied ATM log-normal volatilities, and Panel D of Table 1 reports their averages by moneyness and maturity. Options with short maturities have higher implied volatilities than options with long maturities. Large spikes in the option implied volatilities appear around the end of 1990 and beginning of 1991, at the time of the first Gulf War, around the September 2001 terrorist attack, the second Gulf War in March 2003, and during the financial crisis in 2008.

Among the eleven moneyness intervals, the average implied volatilities are lowest for ATM options. The data exhibit a smirk for several maturities, but for other maturities it is not clear if the smirk pattern is economically significant, or if the data are instead characterized by a smile. These patterns are important with respect to the relative role of return skewness and kurtosis for characterizing the option data. Panel D of Table 2 suggests that modeling kurtosis may be more critical than capturing skewness for crude oil data. This is consistent with the descriptive statistics for the futures data in Table 1.

4. Evidence from Futures Prices

We first discuss how to use maximum likelihood to estimate the models using futures returns. We then present parameter estimates for the four proposed models as well as the benchmark GARCH model. Subsequently we use the parameter estimates to investigate the models' most important implications for option valuation.

4.1 Maximum Likelihood Estimation using Futures Data

We estimate the model parameters using Maximum Likelihood (MLE). The likelihood function for returns depends on the normal and Compound Poisson distributions. The conditional density of the i th returns process in equation (2.8), given that there are $n_{t+1} = j$ jumps occurring between period t and $t+1$, is given by

$$f_t(R_{i,t+1}|n_{t+1} = j) = \frac{1}{\sqrt{2\pi(h_{z,t+1} + j\delta^2)}} \exp\left(-\frac{(R_{i,t+1} - \mu_{i,t+1} - j\theta)^2}{2(h_{z,t+1} + j\delta^2)}\right). \quad (4.1)$$

where $R_{i,t+1} \equiv \log \frac{F_{t+1,T_i}}{F_{t,T_i}}$, and $\mu_{i,t+1} = r_{t+1} + \left(\lambda_z - \frac{1}{2}\right)h_{z,t+1} + (\lambda_y - \xi)h_{y,t+1} + \Delta c(t, t+1, T_i)$.

The conditional probability density of returns can be derived by summing over the number of jumps

$$f_t(R_{i,t+1}) = \sum_{j=1}^{\infty} f_t(R_{i,t+1}|n_{t+1} = j) Pr_t(n_{t+1} = j), \quad (4.2)$$

where $Pr_t(n_{t+1} = j) = (h_{y,t+1})^j \exp(-h_{y,t+1})/j!$ is the probability of having j jumps which is distributed as a Poisson counting process.

We can therefore write the log likelihood function as the summation of the log likelihoods for all eight futures contracts

$$L_{Fut} = \sum_{i=1}^8 \sum_{t=1}^{T-1} \ln(f_t(R_{i,t+1})) \quad (4.3)$$

In estimation we assume that the conditional variance and the jump intensity are equal across maturities. This is clearly a simplifying assumption that will worsen the fit, but it is useful for the purpose of comparison with option-implied estimates.

When implementing maximum likelihood estimation, the summation in (4.2) must be truncated. We truncate the summation at 50 jumps per day. We have experimented with increasing the truncation limit beyond 50 and found that our results are robust.

Equations (2.9) and (2.10) indicate that we need to separately identify the two unobserved shocks z_{t+1} and y_{t+1} and filter the conditional variance $h_{z,t+1}$ and the conditional jump intensity $h_{y,t+1}$ which enter the likelihood function. The structure of the model allows us to do this using an analytical filter, which is discussed in CJO (2012). Using this filter, calculating z_{t+1} and y_{t+1} is straightforward and very fast. It takes less than a second to filter 38,024 futures contracts and about two seconds to filter 283,653 option contracts using Matlab on a standard PC.

4.2 Estimation Results

Table 2 presents the maximum likelihood parameter estimates for the GARCH benchmark model and the four proposed jump models. The results are obtained using all eight futures contracts jointly in estimation for the time period 1990-2008. For each jump model, we separate the parameters into two columns. The parameters with subscript y are reported in the column labeled “Jump”. The parameters with subscript z are reported in the column labeled “Normal”. Under each parameter estimate, we report its standard error calculated using the Hessian matrix. Under “Properties”, we report the implied long-run risk premiums for the normal and jump components, the percent of total variance captured by the normal and the jump component, the average annual volatility, the expected number of jumps per year implied by the parameter estimates, and the log likelihood. Some of these properties are discussed in more detail in Section 4.3 below.

The log-likelihood values of the DVCJ, DVDJ, DVSDJ models are much higher than that of the GARCH model. This is not the case for the CVDJ model, which does not nest the GARCH model. To examine whether the dynamic volatility jump models significantly improve over the GARCH model, we test the null hypothesis of no jumps. To implement this test, we use the standardized likelihood ratio test proposed by Hansen (1992, 1994). A likelihood ratio test of the null hypothesis of no jumps does not have the usual limiting chi-squared distribution because the jump parameters are unidentified under the null. Hansen’s test is able to provide an upper bound to the asymptotic distribution of standardized likelihood ratio statistics, even when conventional regularity conditions (for example due to unidentified parameters) are violated. We calculate Hansen’s test for each of the DVCJ, DVDJ, DVSDJ models compared with GARCH and report the standardized likelihood ratio and the corresponding simulated critical values in Table 3. Using Hansen’s standardized LR test, we find that all three dynamic volatility jump models significantly improve over the GARCH model, suggesting that the null hypothesis of no jumps is rejected. Among the three jump models, the test result for the DVDJ model provides the strongest evidence against

the null. These statistical tests strongly suggest that incorporating jumps in addition to dynamic volatility helps to improve model performance.

The CVDJ model, which has constant conditional variance of the normal component, performs the worst among the four jump models, with the lowest log-likelihood. This suggests that this extended Merton (1976) jump model, which has constant volatility and a GARCH dynamic for the jump intensity is not able to adequately fit the data, which confirms the importance of allowing for time-varying volatility in models for commodity futures. In the CVDJ model, it is not surprising that the jump component of CVDJ accounts for 63% of the total return variance, because the time variation in the return innovation is restricted to the jump intensity. The jump component is relatively more important for this specification because jumps are the only source of heteroskedasticity. In summary, the results for the CVDJ model suggest that jumps are a useful modeling tool, but that modeling time-varying volatility is at least as important. This finding is very similar to results obtained in equity and equity index markets.

The DVCJ model improves model fit significantly by adding a simple constant jump component. For this specification, the average expected number of jumps is given by $E[h_{y,t+1}] = w_y$. The estimate of 0.103 implies that jumps arrive at an annual frequency of 0.103×252 , or approximately 26. This number is much higher than what is usually found in equity index markets, see the summary table in Broadie, Chernov, and Johannes (2007). Most existing estimates in equity index markets find between one and three jumps per year. This suggests that jumps arrive more frequently in the crude oil market. Part of the explanation is that the models identify smaller jumps in crude oil futures as opposed to equity index returns. The estimate of the average jump size θ in the DVCJ model in Table 2 is -0.0069, which is approximately one-fourth of the average jump size in index returns documented in CJO (2012) for a model with constant jump size.

The results for the DVDJ model indicate that allowing for state-dependent jump intensities can further improve model performance. The estimate of k is statistically significant, confirming that the arrival rate of jumps depends on the level of volatility. The mean jump size in the DVDJ model is smaller (in absolute value) than in the DVCJ model and jumps arrive more frequently, with on average 207 jumps per year.

The MLE estimates of the DVSDJ model indicate that there are on average 183 jumps per year. The likelihood for the most general specification, DVSDJ model, further improves on DVDJ. We run a likelihood ratio test to compare DVSDJ with CVDJ and the result is in favor of the unrestricted DVSDJ model.

The results for the DVDJ and DVSDJ models indicate that allowing for time-varying jump intensities can greatly improve model performance. The average jump arrival frequency for the DVDJ and DVSDJ models is significantly lower than for the DVCJ model, but other important model features are similar to the DVCJ model.

4.3 Model Implications

We now further discuss the model properties listed at the bottom of Table 2. We report the decomposition of the total unconditional return variance into the normal and jump components. The total unconditional return variance, σ^2 , is given by

$$\sigma^2 \equiv \sigma_z^2 + (\theta^2 + \delta^2)\sigma_y^2 \quad (4.4)$$

where σ_z^2 and σ_y^2 are computed as the time series averages of $h_{z,t+1}$ and $h_{y,t+1}$. We report the normal contribution and jump contribution to the total return variance in percentages. Overall, the contribution of jumps to the total return variance is very high for the CVDJ model, since jumps are the only source of heteroskedasticity. For the other three models, the DVDJ and DVSDJ models have higher percentages (43.60% and 40.36%) for the jump contribution compared with the DVCJ, which has 15.48% of total variance contributed by the jump component. While the likelihood ratio tests indicate that allowing for time-varying jump intensities is supported statistically, these findings suggest that this model feature is also economically important.

The average variance is very similar across models. The left panels in Figure 4 depict the time path of the conditional variance and clearly indicate that in fact the entire time path is very similar across models, with the exception of the CVDJ model. However, there is one important difference between the models with time-varying intensity (DVDJ and DVSDJ) and the DVCJ model. When the variance increases in 1991 and 2008, the increase is more pronounced for the DVCJ model. The reason for this can be seen in the panels on the right in Figure 4. For the DVDJ and DVSDJ models, there is also a sharp increase in the jump intensity during those crisis periods. The paths of the jump intensity for the DVDJ and DVSDJ models are similar, but the intensity is more variable for the DVSDJ model.

The variations in jump intensities affect the risk premiums, which are depicted in Figure 5. For the DVCJ model in the first row, the risk premium in the middle panel is constant, and all the time variation in the total risk premium in the right panel is due to variation in the normal risk premium. In the case of the DVDJ and DVSDJ models, a large amount of the increase in the total risk premium in 1991 and 2008

is due to the increase in the jump risk premium. This effect is stronger in the more richly parameterized DVSDJ model. For the CVDJ model in the second row, all the time variation in risk premiums is due to the jump risk premium. This clearly does not lead to as much time variation in total risk premiums as for the other models.

Overall, Figure 5 clearly indicates that jump risk premiums are economically important, and that they represent a significant component of the total risk premium. Under “Properties” in Table 2 we also report the averages of the risk premiums over the sample. On average the jump risk premium is large. For the CVDJ model, it is on average larger than the risk premium for the normal component, but this is of course due to the model’s restrictive structure. It is also noteworthy that the average risk premiums are very similar for the DVCJ and DVSDJ models, which have a very different structure. The jump risk premium is relatively smaller in the case of the DVDJ model.

Figure 6 applies the analytical filter to decompose futures returns in the jump and normal component to infer their relative importance. The middle column contains the filtered jump component and the right column contains the filtered normal component. The figures clearly indicate that most of the time, the normal component dominates returns. However, in crises, such as the first Gulf War in late 1991, the jump component explains more of the movement in returns than the normal component. The heteroskedasticity in the normal component is also apparent. The left columns depict the filtered number of jumps n_t occurring each day. We find strong evidence for multiple jumps per day in all jump models, especially during the first Gulf War, when the DVDJ and DVSDJ models indicate 10 jumps per day.

For the purpose of option valuation, the time path of the conditional variance is of paramount importance. However, different models often yield variance paths that are nearly similar, as evidenced by Figure 4. It is therefore of great interest to inspect differences in the conditional third and fourth moments. We now turn to this evidence. The first four conditional moments are given by:

$$E_t(R_{t+1}) \equiv \mu_{t+1} = r_{t+1} + \left(\lambda_z - \frac{1}{2}\right)h_{z,t+1} + (\lambda_y - \xi)h_{y,t+1} + \Delta c(t, t + 1, T) \quad (4.5)$$

$$Var_t(R_{t+1}) = h_{z,t+1} + (\theta^2 + \delta^2)h_{y,t+1} \quad (4.6)$$

$$Skew_t(R_{t+1}) = \frac{\theta(\theta^2 + 3\delta^2)h_{y,t+1}}{(h_{z,t+1} + (\theta^2 + \delta^2)h_{y,t+1})^{\frac{3}{2}}} \quad (4.7)$$

$$Kurt_t(R_{t+1}) = 3 + \frac{(\theta^4 + 6\theta^2\delta^2 + 3\delta^4)h_{y,t+1}}{(h_{z,t+1} + (\theta^2 + \delta^2)h_{y,t+1})^2} \quad (4.8)$$

where $Skew_t(R_{t+1})$ and $Kurt_t(R_{t+1})$ are the conditional skewness and the conditional kurtosis of futures returns respectively. From equation (4.7), it is clear that in presence of jumps, when $h_{y,t+1}$ is positive, the sign of the conditional skewness depends on the sign of the mean jump size θ . Both skewness and kurtosis are critically affected by the parameters θ and δ .

Figure 7 plots the conditional one day ahead skewness in (4.7) and kurtosis in (4.8) for each of the four jump models. The estimated average jump size θ is negative for all four jump models, and therefore the conditional one day ahead skewness is negative. However, skewness is rather small, and interestingly it is smaller for the more flexible models. Conditional kurtosis is of the same order of magnitude for the DVCJ, DVDJ, and DVSDJ models, but contains more sharp peaks for the DVCJ model. Clearly, for a given model outliers in model skewness and kurtosis are related, which is driven by the parameterization.

5. Option Valuation Theory for Crude Oil Futures

We first characterize the risk-neutral dynamics. Subsequently we derive the closed-form option valuation formula.

5.1 The Equivalent Martingale Measure and Risk-Neutral Dynamics

The estimates obtained from futures prices in Section 4 are physical parameters. To value crude oil options, we need return dynamics under the equivalent martingale or risk-neutral measure. In a framework with compound Poisson processes, the futures price can jump to an infinite set of values in a single period, and the equivalent martingale measure is therefore not unique. We proceed by specifying the conditional Radon-Nikodym derivative

$$\frac{\frac{dQ_{t+1}}{dP_{t+1}}}{\frac{dQ_t}{dP_t}} = \frac{\exp(\Lambda_z z_{t+1} + \Lambda_y y_{t+1})}{E_t[\exp(\Lambda_z z_{t+1} + \Lambda_y y_{t+1})]} \quad (5.1)$$

This Radon-Nikodym derivative specifies a risk-neutral probability measure if and only if Λ_z and Λ_y are determined by

$$\Lambda_z + \lambda_z = 0 \quad (5.2)$$

$$\lambda_y - \left(e^{\theta + \frac{\delta^2}{2}} - 1 \right) - e^{\Lambda_y \theta + \frac{\Lambda_y^2 \delta^2}{2}} (1 - e^{(\Lambda_y + 0.5)\delta^2 + \theta}) = 0 \quad (5.3)$$

The futures return process under the risk-neutral dynamic takes the form

$$\log \frac{F_{t+1,T}}{F_{t,T}} = r_{t+1} - \frac{1}{2} h_{z,t+1} - \xi_y(1)^* h_{y,t+1}^* + z_{t+1} + y_{t+1}^* + \Delta c(t, t+1, T) \quad (5.4)$$

with the following variance and jump intensity dynamics

$$h_{z,t+1} = \omega_z + b_z h_{z,t} + \frac{a_z}{h_{z,t}} (z_t - c_z^* h_{z,t})^2 + d_z y_t^* \quad (5.5)$$

$$h_{y,t+1}^* = \omega_y^* + b_y h_{y,t}^* + \frac{a_y^*}{h_{z,t}} (z_t - c_y^* h_{z,t})^2 + d_y^* y_t^* \quad (5.6)$$

where $h_{y,t+1}^* = h_{y,t+1} \Pi$, $\Pi = e^{\Lambda_y \theta + \frac{\Lambda_y^2 \delta^2}{2}}$, $\theta^* = \theta + \Lambda_y \delta^2$, $\xi(1)^* = e^{\theta^* + \frac{\delta^2}{2}} - 1$, $\Lambda_z = -\lambda_z$, $\omega_y^* = \omega_y \Pi$, $a_y^* = \Pi a_y$, $c_z^* = c_z - \Lambda_z$, $c_y^* = c_y - \Lambda_z$, $d_y^* = \Pi d_y$, and $y_{t+1}^* \sim J(h_{y,t+1}^*, \theta^*, \delta^2)$.

The risk neutral dynamic for the GARCH benchmark model in Section 2.1 is a special case of (5.4)-(5.6)

with $h_{y,t+1}^* = y_{t+1}^* = 0$

5.2 Closed-form Option Valuation

Under the risk-neutral measure, the generating function for the asset process in (5.4)-(5.6) takes the following form

$$\begin{aligned} f(\varphi; t, T)^* &\equiv E_t^Q [F_T^\varphi] \\ &= F_{t,T}^\varphi \exp(A1(\varphi; t, T) + B1(\varphi; t, T) h_{z,t+1} + C1(\varphi; t, T) h_{y,t+1}^*) \end{aligned} \quad (5.7)$$

Here we present the analytical solutions to the affine coefficients $A1(\varphi; t, T)$, $B1(\varphi; t, T)$, and $C1(\varphi; t, T)$. Details on the derivation are provided in Appendix B.

$$\begin{aligned} A1(\varphi; t, T) &= \varphi r_{t+1} + A1(\varphi; t+1, T) + B1(\varphi; t+1, T) \omega_z + C1(\varphi; t+1, T) \omega_y^* \\ &\quad - \frac{1}{2} \log(1 - 2B1(\varphi; t+1, T) a_z - 2C1(\varphi; t+1, T) a_y^*) \end{aligned} \quad (5.8)$$

$$\begin{aligned}
B1(\varphi; t, T) &= \varphi\mu_{1z} + B1(\varphi; t + 1, T)(b_z + a_z c_z^{*2}) + C1(\varphi; t + 1, T)a_y^* c_y^{*2} \\
&+ \frac{(\varphi - 2B1(\varphi; t + 1, T)a_z c_z^* - 2C1(\varphi; t + 1, T)a_y^* c_y^*)^2}{2(1 - 2B1(\varphi; t + 1, T)a_z - 2C1(\varphi; t + 1, T)a_y^*)}
\end{aligned} \tag{5.9}$$

$$C1(\varphi; t, T) = b_y C1(\varphi; t + 1, T) + \varphi\mu_{1y} + \xi_y(\mathcal{E})^* \tag{5.10}$$

where $\mu_{1z} = -\frac{1}{2}$, $\mu_{1y} = -\xi_y(1)^*$, $\xi_y(\mathcal{E})^* = e^{\theta^* \mathcal{E}^* + \frac{1}{2} \mathcal{E}^{*2} \delta^2} - 1$,

with $\mathcal{E}^* = \varphi + B1(\varphi; t + 1, T)d_z + C1(\varphi; t + 1, T)d_y^*$ (5.11)

By imposing the restrictions $h_{y,t+1}^* = \omega_y^* = a_y^* = 0$, (5.7)-(5.11) reduces to the generating function for GARCH benchmark model in Section 2.1.

With the risk neutral generating function (5.7), we can value European options using the Fourier inversion method as in Heston (1993), Heston and Nandi (2000), and Duffie, Pan and Singleton (2000). The price of a European call option on a futures contract is given by

$$\begin{aligned}
CO(t, T_{co}, T, K) &= E_t^Q \left[e^{-\int_t^{T_{co}} r(s) ds} (F(T_{co}, T) - K)^+ \right] \\
&= F(t, T) \left(\frac{1}{2} + \frac{1}{\pi} \int_0^\infty \operatorname{Re} \left[\frac{K^{-i\varphi} f^*(i\varphi + 1)}{i\varphi f^*(1)} \right] d\varphi \right) \\
&\quad - e^{-\int_t^{T_{co}} r(s) ds} K \left(\frac{1}{2} + \frac{1}{\pi} \int_0^\infty \operatorname{Re} \left[\frac{K^{-i\varphi} f^*(i\varphi)}{i\varphi} \right] d\varphi \right)
\end{aligned} \tag{5.12}$$

where $CO(t, T_{co}, T, K)$ is the time t price of a European call option expiring at time T_{co} with strike K on a futures contract expiring at time T , and K is the strike price.

6. Estimation using Option Data

We first discuss the loss function used to estimate the model parameters from option data. Subsequently we discuss the empirical results.

6.1 MLE using Option Data

It is possible to use the parameter estimates in Table 2 obtained through MLE estimation on futures data to compute option prices using the option valuation formulae. However, this procedure exclusively uses

historical information and ignores the expectations about the future evolution of the futures prices that are embedded in option prices. We therefore study the models' option valuation performance by maximizing the log-likelihood function for the option contracts to match model option values as closely as possible to observed market prices.

We use a loss function based on implied volatilities, inverting option prices into implied volatilities. This results in a cross-section of market data that is of similar magnitude along the moneyness, maturity, and time-series dimensions. Option prices differ significantly along these dimensions. Define the model error

$$u_k = \sigma_{k,t} - \sigma_{k,t}(O_{k,t}(h_t(\theta^*))) \quad (6.1)$$

where $\sigma_{k,t}$ is the Black (1976) implied volatility of the k^{th} observed option price at time t , and $\sigma_{k,t}(O_{k,t}(h_t(\theta^*)))$ is the implied volatility converted from each computed option price, $O_{k,t}(h_t(\theta^*))$, using the Black (1976) formula.

Assuming normality of the implied volatility errors, the log-likelihood function based on options is

$$L_{Opt} = -\frac{N}{2} \ln(2\pi\sigma_u^2) - \frac{1}{2} \sum_{k=1}^N \frac{u_k^2}{\sigma_u^2} \quad (6.2)$$

where $N = 283,653$ is the total number of option contracts. We estimate parameters based on options data only by maximizing L_{Opt} . We report the optimized likelihoods as well as the corresponding volatility root mean squared error (IVRMSE)

$$IVRMSE = \frac{1}{T} \sqrt{\frac{1}{N} \sum_{t,k} [\sigma_{k,t} - \sigma_{k,t}(O_{k,t}(h_t(\theta^*)))]^2} \quad (6.3)$$

where $T = 4,753$ is the number of days used in our analysis.

Ideally one would fit the model directly to implied Black volatilities. However, since the optimization routine requires computing implied volatility from model prices at every function evaluation, this approach is extremely slow. We follow TS (2009) and fit the model to option prices scaled by their Black (1976) vega, that is, the sensitivities of the option prices to variations in log-normal volatilities. This approach is motivated by the approximation $\sigma_{k,t} \approx O_{k,t}/V_{k,t}$, where $V_{i,t}$ is the Black (1976) vega associated with the i^{th} observed option price at time t . This approximation has been shown to work well in existing work. Thanks to the use of the analytical filter, the quasi-closed form option valuation formula, and the use of the vega-scaled prices, the optimization problem is feasible with our large data sets.

6.2 Empirical Results

Table 4 reports the MLE estimates on crude oil options for the benchmark GARCH model and the four jump models. We report the log likelihood and the IVRMSE for each model at the bottom of the table, as well as a number of important model features implied by the parameter estimates. Note that unlike the parameters in Table 2, these are risk-neutral parameters.

Similar to the estimation results based on crude oil futures data in Table 2, the log-likelihood values for the DVCJ, DVDJ, and DVSDJ models are much higher than that of the GARCH model. The CVDJ model performs the worst among the four jump models. We find that jump models, except for CVDJ model, provide substantial improvements in option pricing performance. Jump models with time-varying intensities, DVDJ and DVSDJ, obtain IVRMSEs of 6.83 and 6.75 respectively and outperform the GARCH model by approximately 6% and 7%. This result further confirms that incorporating time-varying jumps in addition to the dynamic volatilities helps to improve model fit.

The most striking difference between these estimates and the estimates based on futures returns in Table 2 is that the average jump size θ implied by option prices is much larger, and that jumps occur less frequently. These findings suggest that jumps implied by crude oil options are larger and rarer events comparing with those estimated using crude oil futures returns.

7. Estimation using Futures and Options Data

The parameters obtained by minimizing option errors in Section 6 are of substantial interest, and the resulting differences in option fit are a useful indicator of the models' performance. It must also be noted that the exercise in Section 6 does not ignore the underlying futures returns, because volatilities and jump frequencies are filtered from the futures returns. However, the futures returns do not directly enter the loss function.

So while this exercise imposes considerable discipline upon the models, it has nevertheless two important drawbacks. First, if a model is richly parameterized, only fitting the option data may result in overfitting. Second, the price of risk parameters, which are some of the most economically important model parameters, cannot be reliably identified using option data only.

We therefore follow Bates (1996), who suggests that the most stringent test of an option pricing model lies in its ability to jointly fit the option data and the underlying returns. In our case, this means

that we have to construct a loss function that contains a crude oil option component as well as a futures return component.

We first explain how we combine the option data with the underlying futures data to conduct a joint likelihood. We then discuss the parameter estimates, and subsequently we compare the most important model properties with the properties implied by the physical parameters from Table 2.

7.1 The Joint Log Likelihood Function

In previous sections we used MLE to estimate the jump models using futures returns and option implied volatilities respectively. The log-likelihood functions for futures and options are defined in equations (4.3) and (6.2). To jointly estimate the jump models using the option data and the underlying futures data, we maximize the weighted average of the log-likelihoods of futures and options.

The number of option contracts in the data set is much larger than the number of futures contracts. To ensure that joint parameter estimates are not dominated by options, we assign equal weight to each log-likelihood. The resulting weighted joint log-likelihood is

$$L_{Joint} = \frac{M + N}{2} \frac{L_{Fut}}{M} + \frac{M + N}{2} \frac{L_{Opt}}{N} \quad (7.1)$$

where $M=38,024$ is the total number of futures contracts and $N=283,653$ is the total number of option contracts. The joint likelihood function can then be obtained using the results in Sections 4.1 and 6.1.

7.2 Empirical Estimates and Model Implications

Table 5 contains the parameter estimates obtained by maximizing the joint log-likelihood function in (7.1) for the GARCH model and four jump models. At the bottom of the table, we also report the IVRMSE and model properties implied by the parameters such as the long-run risk premium, the percent of total annual variance explained by the normal and the jump component, the average annual volatility, and the expected number of jumps per year.

Similar to the results based on options and the results based on futures, the jump models, except for the CVDJ model, outperform the benchmark GARCH model according to both log-likelihood values and IVRMSE values. The most richly parameterized jump model, DVSDJ, performs best.

The most important conclusion from the parameter estimates is that the structure of the estimated jump processes is very different from the jumps estimated from futures returns in Table 2. Results are more similar to those based on options in Table 4, in the sense that jumps are larger and more infrequent.

The implied expected number of jumps is indeed much smaller than in Table 2. The average number of jumps per year implied by the joint estimation of the DVSDJ model is 0.58, while the average number of jumps calculated from futures returns is 182 per year. For the DVCJ model, we have on average 0.47 jumps per year in Table 5, while in Table 2 we have approximately 26 jumps. The implied variance paths in the left panels of Figure 8 are very similar to the corresponding variance paths in Figure 4. On the contrary, the conditional jump intensities on the right hand side of Figure 8 are of a different order of magnitude than those in Figure 4.

Large and more infrequent jumps are consistent with larger skewness and kurtosis. The estimates of θ are negative for all models, implying negative skewness, but compared to Table 2 they are an order of magnitude larger in absolute value. The estimates of the variance of the jump size δ are larger for the DVCJ and DVSDJ models compared to Table 2. These larger estimates of θ and δ indicate the presence of fatter tails.

Since option prices contain important information about the pricing kernel which is not available from underlying futures returns dynamics, the market prices of risk for the normal component and jump component are of particular interest. The total risk premiums for the DVCJ, DVDJ and DVSDJ models are on average 11.79, 12.81, and 11.77 percent, roughly similar in magnitude, but larger than the implied estimates in Table 2. As a percentage of the total risk premium, the jump risk premium is somewhat smaller than in Table 2, but both the normal and the jump components are economically important in Table 5. Figure 9 plots the resulting time variation in the conditional normal risk premium, the conditional jump risk premium and the total risk premium.

Although the DVCJ model has a higher conditional variance than the other jump models and a lower occurrence of jumps, its total risk premium has a similar magnitude and dynamic as those of the DVDJ and DVSDJ models, but the peaks in the risk premiums are higher. The models with dynamic jump intensities, DVDJ and DVSDJ, have higher jump risk premiums as a percentage of the total risk premium. The time path of the jump risk premiums is similar in the DVDJ and DVSDJ models.

In the models with time-varying jump intensities, DVDJ and DVSDJ, jumps explain approximately 30% of the total variance, while jumps explain 9.71% of the total variance of the DVCJ model. The relatively more prominent role for jumps is consistent with the findings in Table 2, and overall these results confirm the importance of allowing for time-varying jump intensities.

Figure 10 plots the sample paths of the number of jumps, as well as that of the filtered jump component and normal component. Clearly there are far fewer jumps compared to Figure 6. When jumps

happen, they are larger, especially in the case of downward jumps as during the first Gulf war. In those instances, jumps are the dominant component of returns.

Figure 11 plots the time path of conditional skewness and kurtosis. Consistent with the findings of large and infrequent jumps, and the large estimates of θ and δ , skewness and kurtosis are larger in absolute value compared to Table 7. This is especially the case for kurtosis, confirming that for the purpose of modeling options on crude oil futures capturing kurtosis may be more important than capturing skewness.

Table 6 further investigates the differences in fit between the models. We report IVRMSEs and IV bias by moneyness and maturity category. Because of space constraints, we limit ourselves to a comparison of the DVSDJ model and the benchmark GARCH model. For all moneyness and maturity categories in Panel A of Table 6, the average IVRMSE is significantly lower for the DVSDJ model compared to the GARCH model. However, the differences between the models are much larger when considering IV bias in Panel B of Table 6. Since RMSEs reflect model bias and variance, we conclude that the data may be rather noisy, and that some contracts are poorly fit by both models. The much improved bias for the DVSDJ model is therefore very important.

Figure 12 further investigates this by depicting the models' ability to capture the "smiles" and "smirks" in the data. We again limit ourselves to a comparison between the benchmark GARCH model and the DVSDJ model. The red solid line shows the average actual log-normal volatility smiles and smirks. The green dashed line and the blue dotted line show the average of the fitted "smiles" for the DVSDJ model and the GARCH model respectively. Both models are estimated on entire option data. Averages are taken over a maximum of 4,753 daily observations from January 2, 1990 through December 3, 2008. Figure 12 clearly demonstrates that the DVSDJ model fits the implied volatility "smiles" vastly better than the GARCH model for options on all different maturity futures contracts, in line with the bias results in Panel B of Table 6. As maturity increases, the pricing errors of both the GARCH model and the DVSDJ model decrease, suggesting that both models fit long maturity options better.

8. Conclusion

We estimate discrete-time jump models for pricing CME crude oil futures and options on futures. The most general model allows for a heteroskedastic normal innovation and a jump component with time-varying jump intensity. We also investigate three other nested models with jumps, as well as a benchmark

GARCH model that does not contain a jump component. All models are tractable, providing a quasi-analytical option valuation formula, and analytical results for filtering the volatility and jump intensity.

We find strong evidence for the presence of jumps in the crude oil derivatives market, using futures data as well as options data. However, the analysis of futures data favors models with many small jumps, and the presence of multiple jumps per day, especially when market risk is high. The analysis of options data as well as joint estimation of futures and options favors models with infrequent large jumps.

We find strong evidence in favor of time-varying jump intensities. Jump models with dynamic jump intensity dramatically improve model performance. This is the case whether or not futures options are used in estimation. During crisis periods, when market risk is high, jumps occur more frequently.

Jumps account for a large part of the risk premium in crude oil futures, regardless of whether jump intensities are time-varying, and regardless of whether futures or options are used in estimation. Jumps in the crude oil market contribute significantly to the total variation of underlying returns, more so than in equity index markets. The primary purpose of modeling jumps in crude oil markets seems to be to capture the excess kurtosis of the distribution, rather than the skewness.

In future research, we aim to reconcile the finding of many small jumps based on futures data with the finding of infrequent large jumps based on options data.

Appendix

A. The Cost of Carry for Crude Oil

In commodity markets, the arbitrage relationship between futures and spot prices

$$F(t, T) = S(t)e^{r(T-t)} \quad (\text{A.1})$$

may not hold in many cases because of storage costs and convenience yields. Instead, the following relationship applies

$$F(t, T) = S(t)e^{(r-\delta)(T-t)} \quad (\text{A.2})$$

where $c = r - \delta$ is the forward cost of carry, with r denoting the forward interest rate and δ the forward convenience yield net of storage costs.

The convenience yield is generally unobservable. Gibson and Schwartz (1990) provide a method to compute the convenience yield using two futures prices with different maturities. Their procedure relies on the relationship between the futures and the spot price of a commodity (A.2) when there is neither interest rate nor convenience yield uncertainty. Due to the absence of spot crude oil contracts, we use the closest maturity futures contracts prices as proxy for spot prices. This allows us to determine the monthly forward cost of carry by using pairs of different maturity futures prices according to the following formula:

$$c(t, T_i) = \ln \left[\frac{F(t, T_i)}{F(t, T_1)} \right] \quad (\text{A.3})$$

where T_i is the maturity date of the futures contract maturing in i months, with $i = 1, 2, 3, 4, 5, 6, 9, 12$ in our case.

The difference between time t and $t+1$ forward cost of carry for a futures contract maturing in T_i months can be calculated as

$$\Delta c(t, t+1, T_i) = c(t+1, T_i) - c(t, T_i) \quad (\text{A.4})$$

$$\Delta c(t, t+1, T_i) = \ln \left[\frac{F(t+1; T_i)}{F(t+1; T_1)} \right] - \ln \left[\frac{F(t; T_i)}{F(t; T_1)} \right] \quad (\text{A.5})$$

For $i=1$, we have $\Delta c(t, t+1, T_1) = 0$.

B. The Generating Function and the Option Valuation Formula

We solve for the coefficients $A(\varphi; t, T)$, $B(\varphi; t, T)$, and $C(\varphi; t, T)$ in equation (5.7) as in Ingersoll (1987) and Heston and Nandi (2000), utilizing the fact that the conditional moment generating function is exponential affine in the state variables $h_{z,t+1}$ and $h_{y,t+1}^*$.

Since S_T is known at time T , equation (5.7) requires the terminal condition

$$A1(\varphi; T, T) = B1(\varphi; T, T) = C1(\varphi; T, T) = 0 \quad (\text{B.1})$$

Applying the law of iterated expectations to $f(\varphi; t, T)^*$, we get

$$\begin{aligned} f(\varphi; t, T)^* &= E_t^Q[f(\varphi; t+1, T)^*] \\ &= S_t^\varphi E_t^Q[\exp(\varphi R_{t+1} + A1(\varphi; t+1, T) + B1(\varphi; t+1, T)h_{z,t+2} \\ &\quad + C1(\varphi; t+1, T)h_{y,t+2}^*)] \end{aligned} \quad (\text{B.2})$$

We can rewrite the futures return process in (5.4) as

$$R_{t+1} = r_{t+1} + \mu_{1z}h_{z,t+1} + \mu_{1y}h_{y,t+1}^* + z_{t+1} + y_{t+1}^* + \Delta C(t, t+1, T) \quad (\text{B.3})$$

where $\mu_{1z} = -\frac{1}{2}$, $\mu_{1y} = -\xi_y(1)^*$.

Substituting the futures return process in equation (B.3), the conditional normal variance dynamic equation (5.5), and the conditional jump intensity dynamic equation (5.6) into (B.2), we get

$$\begin{aligned} f(\varphi; t, T)^* &= S_t^\varphi E_t^Q \left[\exp(\varphi(r_{t+1} + \mu_{1z}h_{z,t+1} + \mu_{1y}h_{y,t+1}^* + z_{t+1} + y_{t+1}^*) \right. \\ &\quad + A1(\varphi; t+1, T) + B1(\varphi; t+1, T)(\omega_z + b_z h_{z,t+1} \\ &\quad + \frac{a_z}{h_{z,t+1}}(z_{t+1} - c_z h_{z,t+1})^2 + d_z y_{t+1}) + C1(\varphi; t+1, T)(\omega_y^* \\ &\quad \left. + b_y h_{y,t+1}^* + \frac{a_y^*}{h_{z,t+1}}(z_{t+1} - c_y^* h_{z,t+1})^2 + d_y^* y_{t+1}^*)) \right] \end{aligned} \quad (\text{B.4})$$

After rearranging terms through completing squares and following some algebra we get

$$\begin{aligned}
f(\varphi; t, T)^* &= S_t^\varphi E_t^Q \left[\varphi r_{t+1} + A1(\varphi; t+1, T) + B1(\varphi; t+1, T)\omega_z \right. \\
&\quad + C1(\varphi; t+1, T)\omega_y^* + (\varphi\mu_{1z} + (b_z + a_z c_z^2)B1(\varphi; t+1, T))h_{z,t+1} \\
&\quad + (\varphi\mu_{1y} + (b_y + a_y^* c_y^{*2})C1(\varphi; t+1, T))h_{y,t+1}^* \\
&\quad + \left(a_z B1(\varphi; t+1, T) + a_y C1(\varphi; t+1, T) \right) * \frac{z_{t+1}^2}{h_{z,t+1}} \\
&\quad + \left(\varphi - 2a_z c_z B1(\varphi; t+1, T) - 2a_y c_y C1(\varphi; t+1, T) \right) z_{t+1} + (\varphi \\
&\quad \left. + d_z B1(\varphi; t+1, T) + d_y^* C1(\varphi; t+1, T)) y_{t+1}^* \right] \tag{B.5}
\end{aligned}$$

Where we use the following results for normal and Poisson variables

$$E_t^Q[\exp(\alpha z_{t+1}^2 + \beta z_{t+1})] = \exp\left(\frac{\alpha^2 h_{z,t+1}}{2(1-2\beta h_{z,t+1})} - \frac{1}{2}\log(1-2\beta h_{z,t+1})\right) \tag{B.6}$$

$$E_t^Q[\exp(\mathcal{E}y_{t+1}^*)] = \exp(\xi_y(\mathcal{E})^* h_{y,t+1}) \tag{B.7}$$

where $\xi_y(\mathcal{E})^* = e^{\theta^* \mathcal{E}^* + \frac{1}{2} \mathcal{E}^{*2} \delta^2} - 1$.

Substituting (B.6) and (B.7) into (B.5) and subsequently equating terms in the right hand sides of (B.5) and (5.7) gives the analytical solutions for the affine coefficients $A(\varphi; t, T)$, $B(\varphi; t, T)$, and $C(\varphi; t, T)$ in (5.8) and (5.9).

References

- Bakshi, C., Cao, C., and Chen, Z. 1997. Empirical performance of alternative option pricing models. *Journal of Finance* 52, 2003-2049.
- Barone-Adesi, G., Whaley, R., 1987. Efficient analytical approximation of American option values. *Journal of Finance* 42, 301-320.
- Bates, D. 1991. The crash of 87' – was it expected? The evidence from options markets. *Journal of Finance* 46, 1009-1044.
- Bates, D., 1996. Jumps & stochastic volatility: exchange rate processes implicit in Deutschemark options. *Review of Financial studies* 9, 69-107.
- Bates, D., 2000. Post-87 crash fear in S&P500 futures options. *Journal of Econometrics* 94, 181-238.
- Bates, D., 2006. Maximum likelihood estimation of latent affine processes. *Review of Financial Studies* 19, 909-965.
- Black, F., 1976. The pricing of commodity contracts. *Journal of Financial Economics* 3, 167-179.
- Carr, P., and Wu, L., 2004. Time-changed Levy process and option pricing. *Journal of Financial Economics* 17, 113-141.
- Chernov, M., Gallant, R., Ghysels, E., and Tauchen, G., 2003. Alternative models for stock price dynamics. *Journal of Econometrics* 116, 225-257.
- Chiarella, C., Kang, B., Sklibosios, C. N., and To, T. D., 2012. Humps in the volatility structure of the crude oil futures markets: new evidence. University of Technology Sydney, working paper.
- Choi, K. and Hammoudeh, S., 2009. Long memory in oil and refined products markets. *The Energy Journal* 30 (2), 97-116.
- Christie, A. 1982. The stochastic behavior of common stock variances: value, leverage and interest rate effects. *Journal of Financial Economics* 10, 407-432.
- Christoffersen, P., Jacobs, K., and Ornathanalai, C., 2012. Dynamic jump intensities and risk premia: evidence from S&P 500 returns and options. *Journal of Financial Economics*, forthcoming.
- Duan, J. C., 1995. The GARCH option pricing model. *Mathematical Finance* 5, 13-32.
- Duan, J. C., Ritchken, P., and Sun, Z., 2006. Approximating GARCH-jump models, jump-diffusion processes, and option pricing. *Mathematical Finance* 16, 21-52.
- Duffie, D., Pan, J., and Singleton, K., 2000. Transform Analysis and Asset Pricing for Affine Jump-diffusions. *Econometrica* 68, 1343-1376.

Eraker, B., 2004. Do stock prices and volatility jumps? Reconciling evidence from spot and option prices. *Journal of Finance* 59, 1367-1403.

Eraker, B., Johannes, M., and Polson, N., 2003. The impact of jumps in volatility and returns. *Journal of Finance* 58, 1269-1300.

Gibson, R., Schwartz E. S., 1990. Stochastic convenience yield and the pricing of oil contingent claims. *Journal of Finance* 45, 959-976.

Hamilton, J. D., Wu, J. C., 2012. Risk premia in crude oil futures prices. Working paper, University of California, San Diego, University of Chicago.

Hansen, B. E., 1992. The Likelihood Ratio Test under Non-standard Conditions: Testing the Markov Trend Model of GNP. *Journal of Applied Econometrics* 7, S61-S82.

Hansen, B. E., 1994. Autoregressive conditional density estimation. *International Economic Review* 35, 705-730.

Heston, S., 1993. A closed-form solution for options with stochastic volatility with applications to bond and currency options. *Review of Financial Studies* 6, 327-343.

Heston, S., Nandi, S., 2000. A closed-form GARCH option pricing model. *Review of Financial Studies* 13, 585-626.

Ingersoll, J., 1987. *Theory of financial decision making*, Rowman and littlefield, Totowa, N.J.

Larsson, K., Nossman, M., 2010. Jumps and stochastic volatility in oil prices: time series evidence. Working paper, Lund University.

Lee, M. C. and Cheng W. H., 2007. Correlated jumps in crude oil and gasoline during the Gulf War. *Atlantic Economic Journal* 19 (4), 107-132.

Li, H., Wells, M., and Yu, C., 2007. A Bayesian analysis of return dynamics with Levy jumps. *Review of Financial Studies* 21, 2345-2378.

Litzenberger, R., and Rabinowitz, N., 1995. Backwardation in Oil Futures Markets: Theory and Empirical Evidence. *Journal of Finance* 50, 1517-1545.

Liu, H., Lee, M., and Chang, C., 2009. The role of SGT distribution in value-at risk estimation: evidence from the WTI crude oil market. *Investment Management and Financial Innovations* 6, 86-95.

Maheu, J., and McCurdy, T., 2004, News arrival, jump dynamics and volatility components for individual stock returns. *Journal of Finance* 59, 755-793.

Merton, R., 1976. Option pricing when underlying stock returns are discontinuous. *Journal of Financial Economics* 3, 125-144.

- Ornathanalai, C., 2012. Levy jump risk: Evidence from options and returns. Working paper, Georgia Institute of Technology.
- Pan, J., 2002. The jump-risk premia implicit in options: evidence from an integrated time-series study. *Journal of Financial Economics* 63, 3-50.
- Pan, X. N., 2011. Investor beliefs and state price densities in the crude oil market. Working paper, McGill University.
- Santa-Clara, P., Yan, S., 2010. Crashes, volatility, and the equity premium: lessons from S&P500 options. *Review of Economics and Statistics* 92, 435-451.
- Shih, T., Yu, H., 2009. Probability distribution of return and volatility in crude oil market. Working paper, Mingdao University.
- Trolle, A. B., Schwartz, E. S., 2009. Unspanned stochastic volatility and the pricing of commodity derivatives. *Review of Financial Studies* 22, 4423-4461.

Table 1. Summary Statistics

We report summary statistics for crude oil futures returns and options. M1 (M2, M3, M4, M5, M6) refers to futures contracts with expiration in 1 (2, 3, 4, 5, 6) months; Q1 and Q2 refer to the next two futures contracts with expiration in either March, June, September or December. Moneyness is defined as the option strike divided by the price of the underlying futures contract. The data spans 4,753 trading days from January 2, 1990 to December 3, 2008.

Panel A. Historical Moments of Futures Returns

	Maturity								Average
	M1	M2	M3	M4	M5	M6	Q1	Q2	
Mean	0.0002	0.0002	0.0002	0.0002	0.0002	0.0002	0.0002	0.0002	0.0002
Variance	0.0005	0.0004	0.0004	0.0003	0.0003	0.0003	0.0003	0.0002	0.0003
Skewness	-1.25	-1.16	-1.01	-0.94	-0.87	-0.80	-0.71	-0.51	-0.91
Kurtosis	23.38	19.50	15.91	14.46	13.21	12.01	10.98	8.66	14.77

Panel B. Average Number of Option Contracts

		Maturity								All
	Moneyness	M1	M2	M3	M4	M5	M6	Q1	Q2	
Puts	0.78-0.82	443	2122	2765	2867	2790	2559	2504	1738	17788
	0.82-0.86	1087	2907	3340	3424	3293	2974	2883	2007	21915
	0.86-0.90	1985	3647	3960	4065	3897	3474	3217	2335	26580
	0.90-0.94	3080	4309	4470	4262	4056	3592	3345	2434	29548
	0.94-0.98	4000	4607	4472	4190	4070	3635	3416	2559	30949
	0.98-1.02	4410	4527	4400	4116	3958	3505	3355	2482	30753
Calls	1.02-1.06	4001	4605	4470	4259	3973	3464	3249	2337	30358
	1.06-1.10	3136	4362	4405	4155	3925	3473	3161	2153	28770
	1.10-1.14	2209	3714	4196	4042	3683	3151	3116	1994	26105
	1.14-1.18	1404	3135	3482	3574	3368	2877	2877	1845	22562
	1.18-1.22	815	2547	3010	2819	2674	2367	2366	1727	18325
All		26570	40482	42970	41773	39687	35071	33489	23611	283653

Panel C. Average Option Prices

		Maturity								
	Moneyness	M1	M2	M3	M4	M5	M6	Q1	Q2	All
Puts	0.78-0.82	0.27	0.31	0.45	0.58	0.72	0.89	1.11	1.58	0.74
	0.82-0.86	0.26	0.40	0.59	0.75	0.92	1.11	1.36	1.86	0.91
	0.86-0.90	0.31	0.55	0.78	0.95	1.12	1.33	1.67	2.15	1.11
	0.90-0.94	0.42	0.76	1.04	1.29	1.50	1.78	2.10	2.64	1.44
	0.94-0.98	0.66	1.14	1.51	1.82	2.02	2.31	2.67	3.13	1.91
	0.98-1.02	1.08	1.69	2.09	2.43	2.64	2.96	3.36	3.90	2.52
Calls	1.02-1.06	0.69	1.20	1.59	1.89	2.14	2.43	2.86	3.52	2.04
	1.06-1.10	0.48	0.86	1.18	1.45	1.66	1.91	2.30	2.96	1.60
	1.10-1.14	0.37	0.68	0.91	1.13	1.30	1.53	1.83	2.51	1.28
	1.14-1.18	0.33	0.54	0.78	0.94	1.06	1.23	1.53	2.14	1.07
	1.18-1.22	0.32	0.44	0.65	0.86	0.96	1.11	1.33	1.71	0.92
	All	0.47	0.78	1.05	1.28	1.46	1.69	2.01	2.56	1.41

Panel D. Average Implied Log-Normal Volatilities

		Maturity								
	Moneyness	M1	M2	M3	M4	M5	M6	Q1	Q2	All
Puts	0.78-0.82	0.57	0.44	0.40	0.37	0.36	0.34	0.32	0.30	0.39
	0.82-0.86	0.47	0.41	0.38	0.35	0.33	0.32	0.30	0.29	0.36
	0.86-0.90	0.43	0.38	0.35	0.33	0.31	0.30	0.29	0.27	0.33
	0.90-0.94	0.39	0.35	0.33	0.31	0.30	0.30	0.28	0.27	0.32
	0.94-0.98	0.35	0.33	0.32	0.31	0.30	0.29	0.28	0.26	0.30
	0.98-1.02	0.33	0.33	0.32	0.31	0.29	0.29	0.27	0.26	0.30
Calls	1.02-1.06	0.35	0.33	0.32	0.31	0.29	0.29	0.27	0.26	0.30
	1.06-1.10	0.38	0.34	0.32	0.31	0.29	0.29	0.27	0.26	0.31
	1.10-1.14	0.41	0.36	0.33	0.31	0.30	0.29	0.27	0.26	0.32
	1.14-1.18	0.45	0.39	0.36	0.33	0.30	0.29	0.27	0.26	0.33
	1.18-1.22	0.50	0.40	0.37	0.35	0.32	0.31	0.28	0.26	0.35
	All	0.42	0.37	0.34	0.33	0.31	0.30	0.28	0.27	0.33

Table 2. MLE Estimates using Crude Oil Futures Returns, 1990 – 2008

We report estimation results from MLE estimation on daily crude oil futures returns from January 2, 1990 to December 3, 2008. Columns labeled “Normal” contain estimates of the parameters governing the normal component; columns labeled “Jump” contain parameters governing the jump component. Reported in parentheses are standard errors computed using the Hessian matrix.

Parameters	GARCH		DVCJ		CVDJ		DVDJ		DVSDJ	
	<u>Normal</u>	<u>Normal</u>	<u>Jump</u>	<u>Normal</u>	<u>Jump</u>	<u>Normal</u>	<u>Jump</u>	<u>Normal</u>	<u>Jump</u>	
λ	7.31E-01 (1.72E-03)	5.27E-01 (2.22E-04)	1.52E-03 (2.32E-06)	9.93E-01 (5.41E-03)	9.75E-04 (2.87E-06)	1.08E+00 (3.10E-03)	1.11E-04 (4.31E-08)	7.66E-01 (1.42E-03)	2.17E-04 (3.72E-08)	
w	-1.03E-05 (1.06E-08)	-1.50E-05 (3.31E-08)	1.03E-01 (4.69E-04)	1.85E-04 (5.28E-07)	5.52E-03 (7.17E-06)	-1.45E-05 (5.66E-08)		-1.45E-05 (1.21E-08)	3.46E-02 (6.13E-05)	
a	2.01E-05 (4.45E-08)	2.56E-05 (1.91E-07)			3.30E-03 (6.46E-06)	2.81E-05 (7.61E-08)		2.86E-05 (2.49E-08)	2.98E-02 (4.89E-05)	
b	9.78E-01 (1.14E-03)	9.81E-01 (1.18E-03)			9.71E-01 (1.47E-03)	9.89E-01 (8.17E-04)		9.85E-01 (1.12E-03)	5.52E-01 (1.26E-03)	
c	1.03E+01 (2.14E-02)	6.32E+00 (9.44E-03)			2.81E+00 (7.23E-03)	9.04E+00 (1.96E-02)		9.90E+00 (1.71E-02)	1.82E+02 (4.53E-01)	
d		-3.71E-04 (6.52E-07)			1.75E-03 (2.29E-06)	5.27E-05 (8.45E-08)		5.85E-05 (2.08E-07)	8.65E-02 (1.28E-04)	
θ			-6.87E-03 (1.29E-05)		-8.99E-03 (3.19E-05)		-2.08E-03 (1.67E-06)		-2.18E-03 (6.97E-06)	
δ			2.54E-02 (5.02E-05)		3.34E-02 (4.92E-05)		1.55E-02 (1.71E-05)		1.59E-02 (2.24E-05)	
k							3.14E+03 (7.72E+00)			
Properties										
Risk Premium (%)	9.18	5.16	3.94	4.63	6.49	7.10	2.30	5.33	3.97	
% of Annual Variance	100.00	84.52	15.48	36.93	63.07	56.40	43.60	59.64	40.36	
Ave. Annual Volatility	0.35		0.34		0.36		0.34		0.34	
Exp. No. of Jumps/Yr.			25.9		66.5		206.5		182.8	
Log-Likelihood	11682		11830		11544		11841		11850	

Table 3. Hansen's Standardized Likelihood Ratio test

We report Hansen's Standardized Likelihood Ratio test and the corresponding simulated critical values for the discrete-time DVCJ, DVDJ, and DVSDJ jump models. Under the null hypothesis there are no jumps. The log likelihoods are calculated using daily crude oil futures returns from January 2, 1990 to December 3, 2008. *, **, *** and **** represents significance at the 20%, 10%, 5% and 1% level or better.

Models	DVCJ	DVDJ	DVSDJ
Hansen's standardized LR test	4.5946****	11.5006****	5.3905****
Simulated 20% critical value	1.4400	1.5399	1.6021
Simulated 10% critical value	1.8731	1.9776	2.0262
Simulated 5% critical value	2.1269	2.4070	2.3480
Simulated 1% critical value	2.7016	3.0147	3.1183

Table 4. MLE Estimates using Crude Oil Options, 1990-2008

We report risk-neutral estimation results from MLE estimation on daily crude oil options from January 2, 1990 to December 3, 2008. Columns labeled “Normal” contain estimates of the parameters governing the normal component; columns labeled “Jump” contain parameters governing the jump component. Reported in parentheses are standard errors computed using the Hessian matrix.

Parameters	GARCH	DVCJ		CVDJ		DVDJ		DVSDJ	
	<u>Normal</u>	<u>Normal</u>	<u>Jump</u>	<u>Normal</u>	<u>Jump</u>	<u>Normal</u>	<u>Jump</u>	<u>Normal</u>	<u>Jump</u>
w*	-6.23E-06 (4.03E-07)	-1.04E-05 (1.40E-06)	7.68E-04 (3.76E-05)	2.09E-04 (1.90E-05)	5.96E-04 (4.55E-05)	-9.04E-06 (1.04E-06)		-8.98E-06 (5.27E-07)	-6.63E-05 (1.01E-05)
a*	9.22E-06 (5.91E-07)	1.26E-05 (2.19E-06)			2.05E-03 (1.30E-04)	1.17E-05 (1.09E-06)		1.17E-05 (2.01E-06)	8.41E-05 (6.10E-06)
b	9.76E-01 (1.40E-02)	9.83E-01 (5.07E-03)			9.71E-01 (1.53E-02)	9.84E-01 (5.52E-03)		9.83E-01 (9.59E-03)	9.83E-01 (1.31E-02)
c*	3.27E+00 (5.46E-01)	2.56E+01 (1.34E+00)			1.10E+01 (1.63E-01)	6.80E+00 (7.43E-01)		9.63E+00 (7.51E-01)	2.08E+00 (1.91E-01)
d*		8.56E-05 (3.88E-05)			9.65E-05 (7.47E-06)	6.54E-04 (6.54E-05)		5.67E-05 (7.83E-06)	2.58E-04 (2.90E-05)
θ *			-2.17E-02 (2.75E-03)		-2.14E-02 (1.94E-03)		-2.64E-01 (7.34E-03)		-2.63E-01 (2.83E-02)
δ			2.49E-01 (6.36E-02)		3.59E-02 (6.78E-04)		1.44E-02 (1.56E-03)		1.38E-03 (6.59E-05)
k*							7.07E+00 (3.15E-01)		
<u>Properties</u>									
% of Annual Variance	100.00	89.10	10.90	56.37	43.63	66.86	33.14	65.78	34.22
Ave. Annual Volatility	0.29		0.33		0.31		0.37		0.37
Exp. No. of Jumps/Yr.			0.19		23.36		0.65		0.47
RMSE	7.23		7.13		9.84		6.83		6.75
Log-Likelihood	335441		346577		255322		358555		359739

Table 5. Joint MLE Estimates using Crude Oil Futures and Options, 1990-2008

We report estimation results from MLE estimation using daily crude oil futures and options from January 2, 1990 to December 3, 2008. Reported in parentheses are standard errors computed using the Hessian matrix.

Parameters	GARCH		DVCJ		CVDJ		DVDJ		DVSDJ	
	<u>Normal</u>	<u>Normal</u>	<u>Jump</u>	<u>Normal</u>	<u>Jump</u>	<u>Normal</u>	<u>Jump</u>	<u>Normal</u>	<u>Jump</u>	
λ	1.40E+00 (3.25E-01)	1.09E+00 (7.36E-02)	2.99E-02 (2.11E-03)	2.05E+00 (2.08E-01)	2.90E-03 (2.36E-04)	1.14E+00 (4.46E-04)	4.11E-02 (1.04E-05)	9.61E-01 (2.12E-02)	5.44E-02 (1.68E-03)	
w	-6.28E-06 (5.96E-08)	-1.04E-05 (6.46E-07)	1.88E-03 (6.87E-05)	9.89E-05 (1.78E-05)	2.88E-03 (1.57E-04)	-9.04E-06 (4.82E-09)		-1.33E-05 (1.42E-06)	-1.82E-05 (9.63E-07)	
a	9.59E-06 (6.88E-08)	1.27E-05 (5.39E-07)			2.56E-03 (2.02E-04)	1.17E-05 (6.38E-09)		1.66E-05 (1.52E-06)	1.07E-05 (7.15E-07)	
b	9.87E-01 (1.27E-04)	9.83E-01 (4.25E-03)			9.61E-01 (8.11E-03)	9.84E-01 (2.56E-05)		9.73E-01 (1.32E-02)	9.61E-01 (5.82E-02)	
c	2.07E+00 (5.24E-01)	2.35E+01 (2.11E-01)			1.80E+01 (9.67E-01)	5.16E+00 (1.10E-03)		2.35E+01 (4.30E-01)	1.61E+02 (4.36E+00)	
d		8.01E-05 (6.16E-06)			9.43E-05 (8.06E-06)	1.30E-04 (7.86E-08)		7.91E-05 (1.08E-05)	9.09E-06 (6.40E-07)	
θ			-2.47E-02 (1.54E-03)		-2.00E-02 (2.06E-03)		-2.64E-01 (1.18E-04)		-1.07E-02 (1.07E-03)	
δ			1.44E-01 (1.24E-02)		3.59E-02 (2.59E-03)		1.44E-02 (5.86E-06)		2.63E-01 (8.70E-03)	
k							6.00E+00 (3.65E-03)			
Properties										
Risk Premium (%)	14.07	10.37	1.42	5.10	10.55	10.53	2.28	8.60	3.17	
% of Annual Variance	100.00	90.29	9.71	28.88	71.12	70.40	29.60	68.86	31.14	
Ave. Annual Volatility	0.32		0.32		0.29		0.36		0.36	
Exp. No. of Jumps/Yr.			0.47		37.17		0.56		0.58	
RMSE	7.26		7.06		10.05		6.86		6.77	
Log-Likelihood	245031		247921		187131		252327		257467	

Table 6. IVRMSEs and IV Bias for Crude Oil Options by Moneyness and Maturity

We report the option implied volatility root mean squared errors (IVRMSEs) and the implied volatility bias within each moneyness-maturity category for the GARCH and DVSDJ models. The models are estimated using daily crude oil returns and options jointly for the period January 2, 1990 to December 3, 2008. The pricing errors are defined as the difference between fitted and actual implied volatilities and reported in percentage. M1 (M2, M3, M4, M5, M6) means option contracts with expiration in next (2, 3, 4, 5, 6) month; Q1 and Q2 refers to the next two option contracts with expiration in either March, June, September or December. Moneyness is defined as the option strike divided by the price of the underlying futures contract.

Panel A. IVRMSEs for Crude Oil Options by Moneyness and Maturity

	Moneyness	Model	Maturity							
			M1	M2	M3	M4	M5	M6	Q1	Q2
Puts	0.78-0.82	GARCH	12.85	9.01	7.89	7.12	6.75	6.18	5.75	5.98
		DVSDJ	9.12	7.87	7.05	6.33	6.14	5.76	5.54	5.68
	0.82-0.86	GARCH	10.88	9.01	8.23	7.56	7.07	6.17	5.88	6.17
		DVSDJ	8.01	7.26	6.96	6.60	6.38	5.87	5.55	5.71
	0.86-0.90	GARCH	9.81	8.82	8.09	7.49	7.02	6.31	6.03	6.48
		DVSDJ	7.52	7.19	7.04	6.71	6.42	5.98	5.76	6.26
	0.90-0.94	GARCH	8.74	8.36	7.61	6.96	6.82	6.22	6.06	6.57
		DVSDJ	7.44	7.27	6.76	6.28	6.23	5.80	5.66	5.69
	0.94-0.98	GARCH	8.42	8.15	7.56	7.06	6.43	6.13	6.13	6.93
		DVSDJ	7.91	7.42	6.90	6.40	5.86	5.59	5.52	5.77
	0.98-1.02	GARCH	8.41	8.09	7.53	7.11	6.32	6.14	6.32	6.98
		DVSDJ	8.38	7.68	7.05	6.54	5.74	5.44	5.57	5.84
	1.02-1.06	GARCH	8.29	8.26	7.53	7.01	6.40	6.28	6.38	6.93
		DVSDJ	8.14	7.84	7.03	6.42	5.72	5.58	5.48	5.58
	1.06-1.10	GARCH	8.49	8.50	7.68	7.09	6.56	6.33	6.38	7.00
		DVSDJ	7.85	7.92	7.06	6.49	5.86	5.60	5.36	5.70
Calls	1.10-1.14	GARCH	9.24	8.68	7.82	7.17	6.69	6.40	6.62	7.21
		DVSDJ	7.97	7.87	7.25	6.53	5.93	5.77	5.53	6.01
	1.14-1.18	GARCH	10.29	9.01	8.13	7.38	6.64	6.61	6.87	7.72
		DVSDJ	8.53	7.95	7.31	6.75	6.05	5.95	5.88	6.04
	1.18-1.22	GARCH	11.83	9.33	8.21	7.50	6.76	6.71	6.44	7.91
		DVSDJ	9.44	8.23	7.40	6.87	6.01	5.87	5.47	5.71

Panel B. IV Bias for Crude Oil Options by Moneyness and Maturity

	Moneyness	Model	Maturity							
			M1	M2	M3	M4	M5	M6	Q1	Q2
Puts	0.78-0.82	GARCH	-13.82	-7.65	-5.95	-4.72	-3.80	-3.47	-2.24	-2.24
		DVSDJ	-3.89	0.40	0.47	0.29	0.11	-0.19	-0.32	-1.29
	0.82-0.86	GARCH	-11.51	-7.18	-5.17	-3.64	-2.70	-2.29	-1.14	-0.57
		DVSDJ	-1.98	-0.48	-0.28	0.09	0.15	0.05	-0.10	-0.69
	0.86-0.90	GARCH	-8.59	-5.77	-3.76	-2.30	-1.38	-0.94	-0.15	0.76
		DVSDJ	-2.53	-1.41	-0.55	-0.02	0.22	0.34	0.24	0.43
	0.90-0.94	GARCH	-5.77	-4.00	-2.73	-1.66	-0.89	-0.48	0.48	1.48
		DVSDJ	-3.11	-1.79	-0.95	-0.33	0.00	0.16	0.29	0.25
	0.94-0.98	GARCH	-3.36	-3.01	-2.22	-1.40	-0.48	-0.01	0.95	2.37
		DVSDJ	-3.48	-2.24	-1.39	-0.84	-0.28	-0.04	0.23	0.70
	0.98-1.02	GARCH	-2.07	-2.68	-1.98	-1.20	-0.24	0.24	1.30	2.27
		DVSDJ	-3.72	-2.63	-1.75	-1.16	-0.48	-0.22	0.30	0.77
1.02-1.06	GARCH	-2.93	-2.65	-1.90	-0.97	-0.04	0.53	1.44	2.46	
	DVSDJ	-3.91	-2.62	-1.77	-1.08	-0.49	-0.04	0.20	0.30	
1.06-1.10	GARCH	-4.80	-3.16	-2.01	-1.04	-0.04	0.41	1.54	2.37	
	DVSDJ	-3.64	-2.46	-1.59	-1.04	-0.49	-0.30	0.08	0.25	
Calls	1.10-1.14	GARCH	-7.03	-4.52	-2.55	-1.33	-0.03	0.36	1.71	2.28
		DVSDJ	-3.65	-2.49	-1.51	-1.03	-0.31	-0.29	0.35	0.44
	1.14-1.18	GARCH	-9.50	-5.66	-3.68	-1.93	-0.50	0.25	1.49	2.67
		DVSDJ	-3.58	-2.14	-1.69	-1.03	-0.43	-0.16	0.30	0.46
	1.18-1.22	GARCH	-12.40	-6.39	-4.38	-3.04	-1.36	-0.31	1.07	2.45
		DVSDJ	-4.68	-1.53	-1.45	-1.44	-0.85	-0.49	0.02	0.13

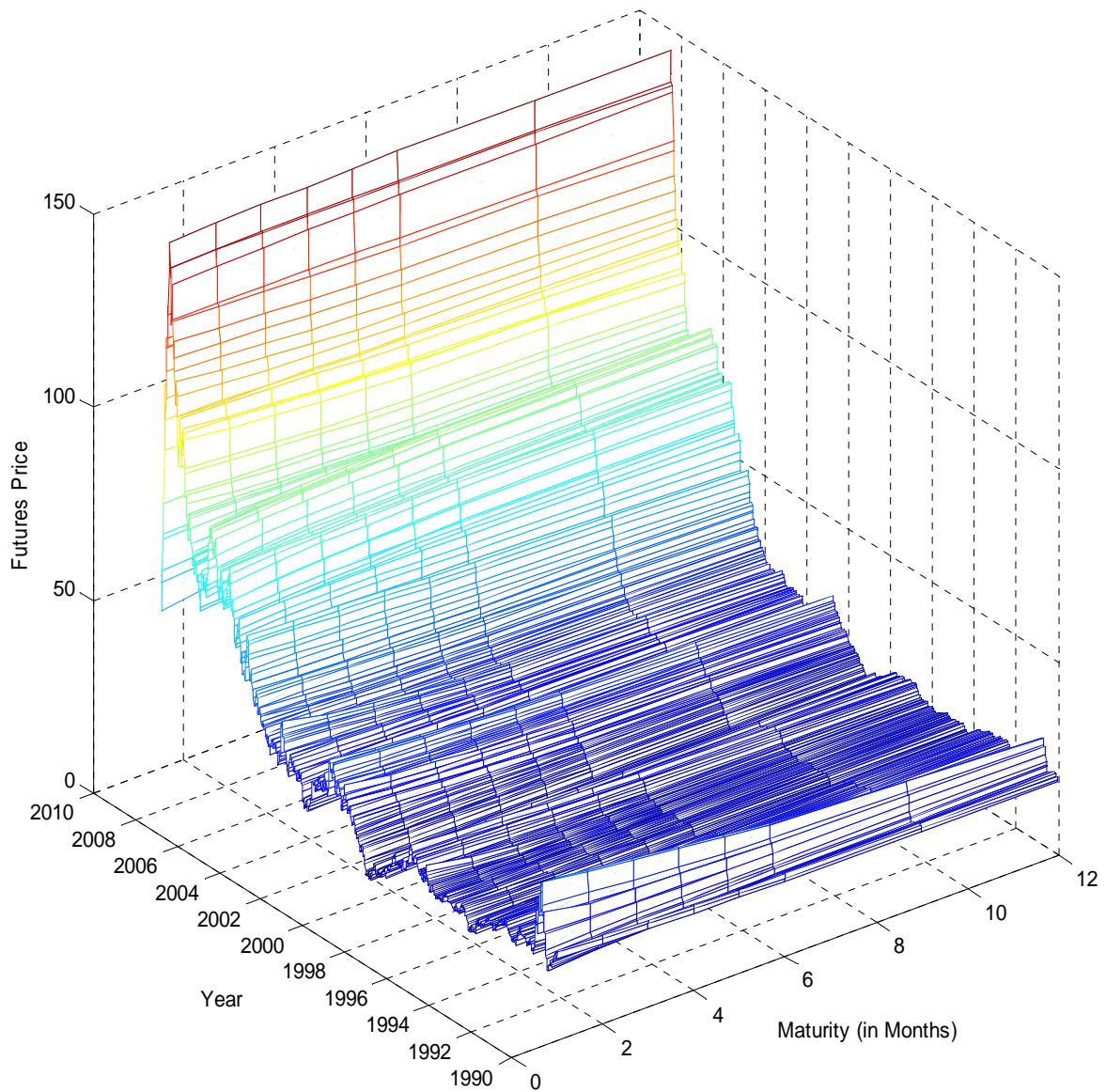


Figure 1. Prices of Futures Contracts

We plot the prices of the M1, M2, M3, M4, M5, M6, Q1, and Q2 futures contracts. The data spans 4,753 trading dates from January 2, 1990 to December 3, 2008. To avoid cluttering the figure, we only display the futures term structures on Wednesdays.

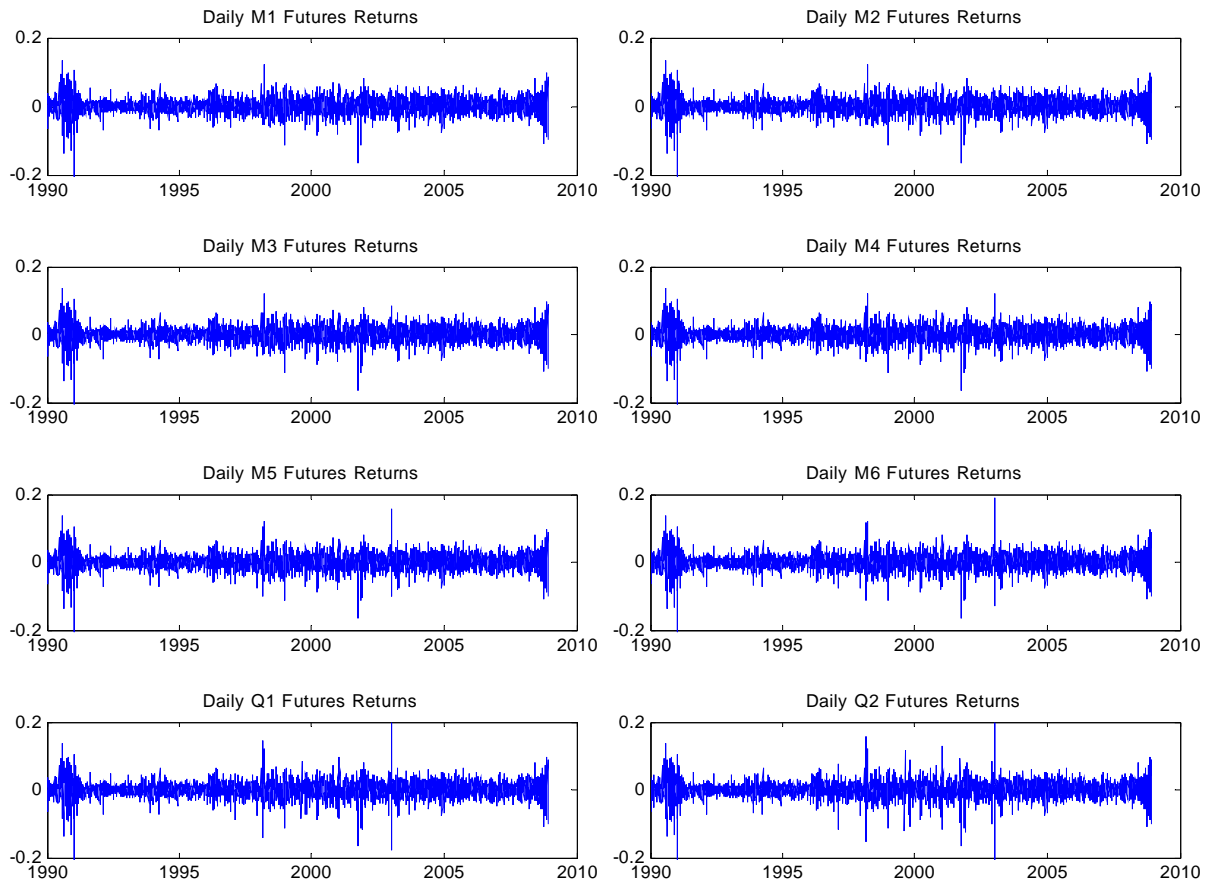


Figure 2. Daily Futures Returns

We plot daily futures returns, $\log \frac{F_{t+1,T}}{F_{t,T}}$, on the M1, M2, M3, M5, M6, Q1, and Q2 futures contracts. The data spans 4753 trading dates from January 2, 1990 to December 3, 2008.

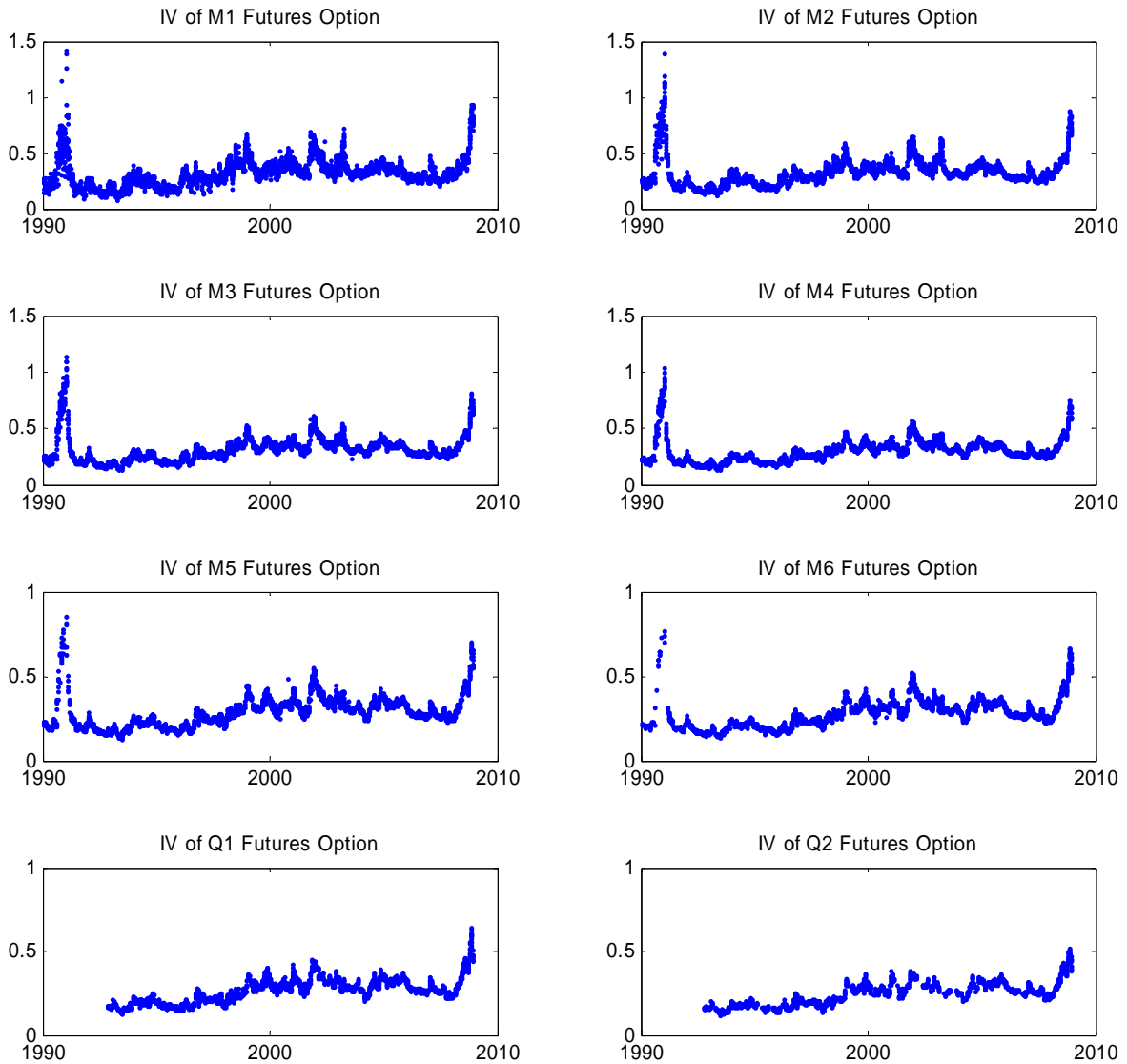


Figure 3. Implied Log-Normal ATM Volatility of Futures Options

We plot implied log-normal ATM volatilities of options on the M1, M2, M3, M5, M6, Q1, and Q2 futures contracts. Implied volatilities are computed from option prices by inverting the Barone-Adesi and Whaley (1987) formula. The data spans 4,753 trading dates from January 2, 1990 to December 3, 2008.

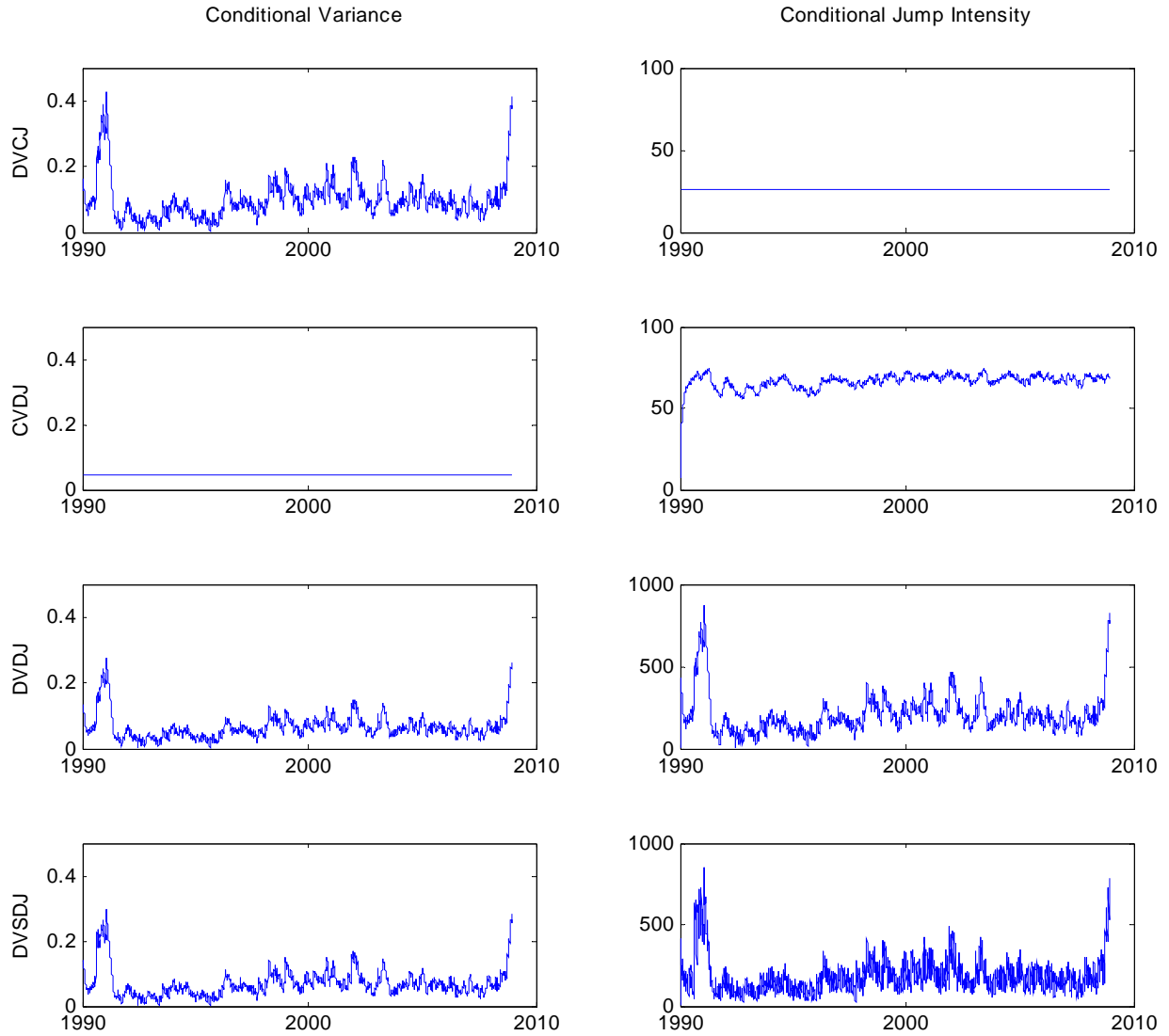


Figure 4. Conditional Variance and Jump Intensity Estimated Using Futures Contracts

We plot the annualized conditional variance, $h_{z,t+1}$, in the left column and the annualized conditional jump intensity, $h_{y,t+1}$, in the right column for four jump models.

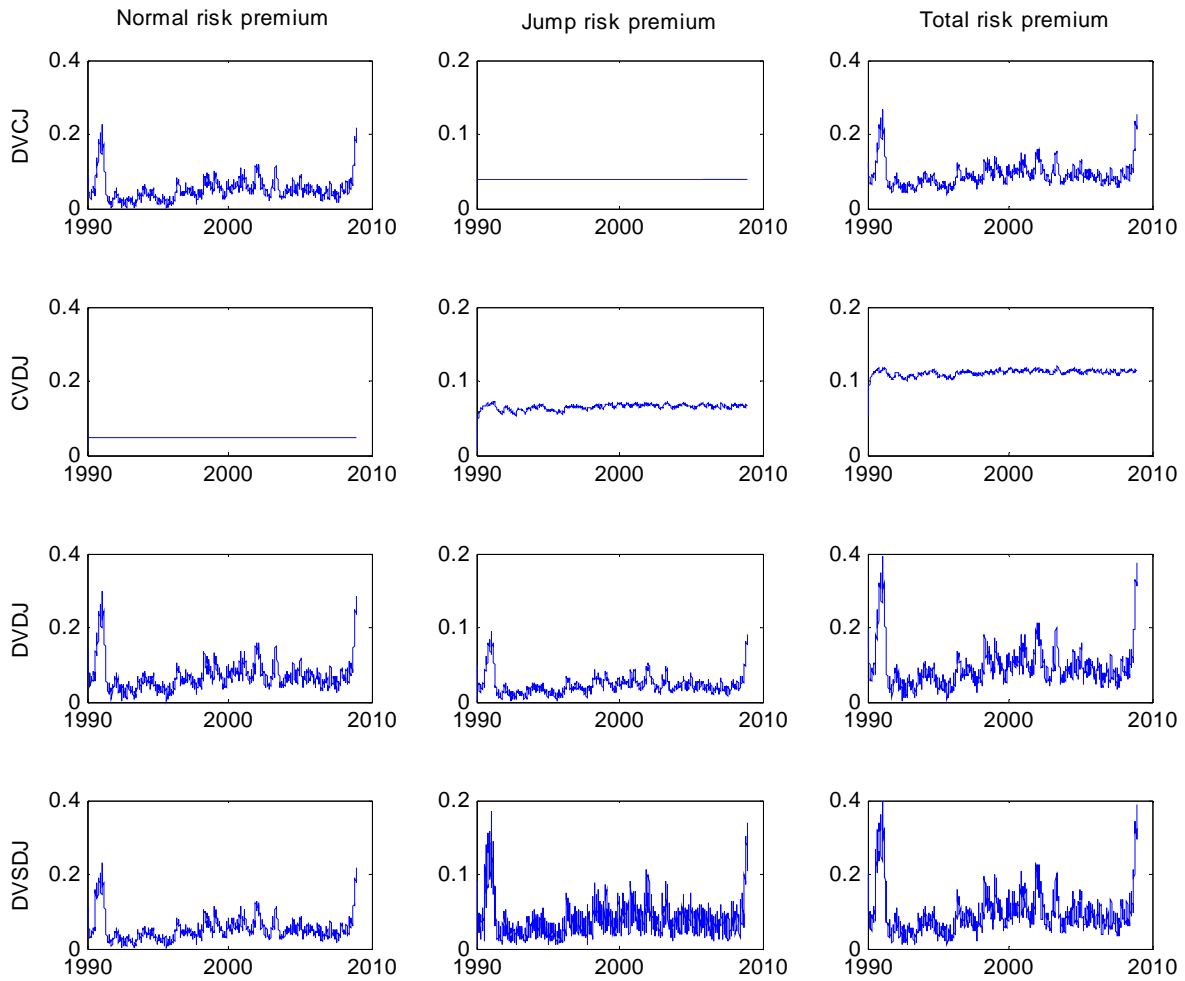


Figure 5. Risk Premiums Estimated Using Futures Contracts

We plot the normal risk premium, $\gamma_{z,t} \equiv \lambda_z h_{z,t}$, in the left column, the jump risk premium, $\gamma_{y,t} \equiv \lambda_y h_{y,t}$, in the middle column, and the total risk premium, $\gamma_t \equiv \lambda_z h_z + \lambda_y h_y$, in the right column for four jump models.

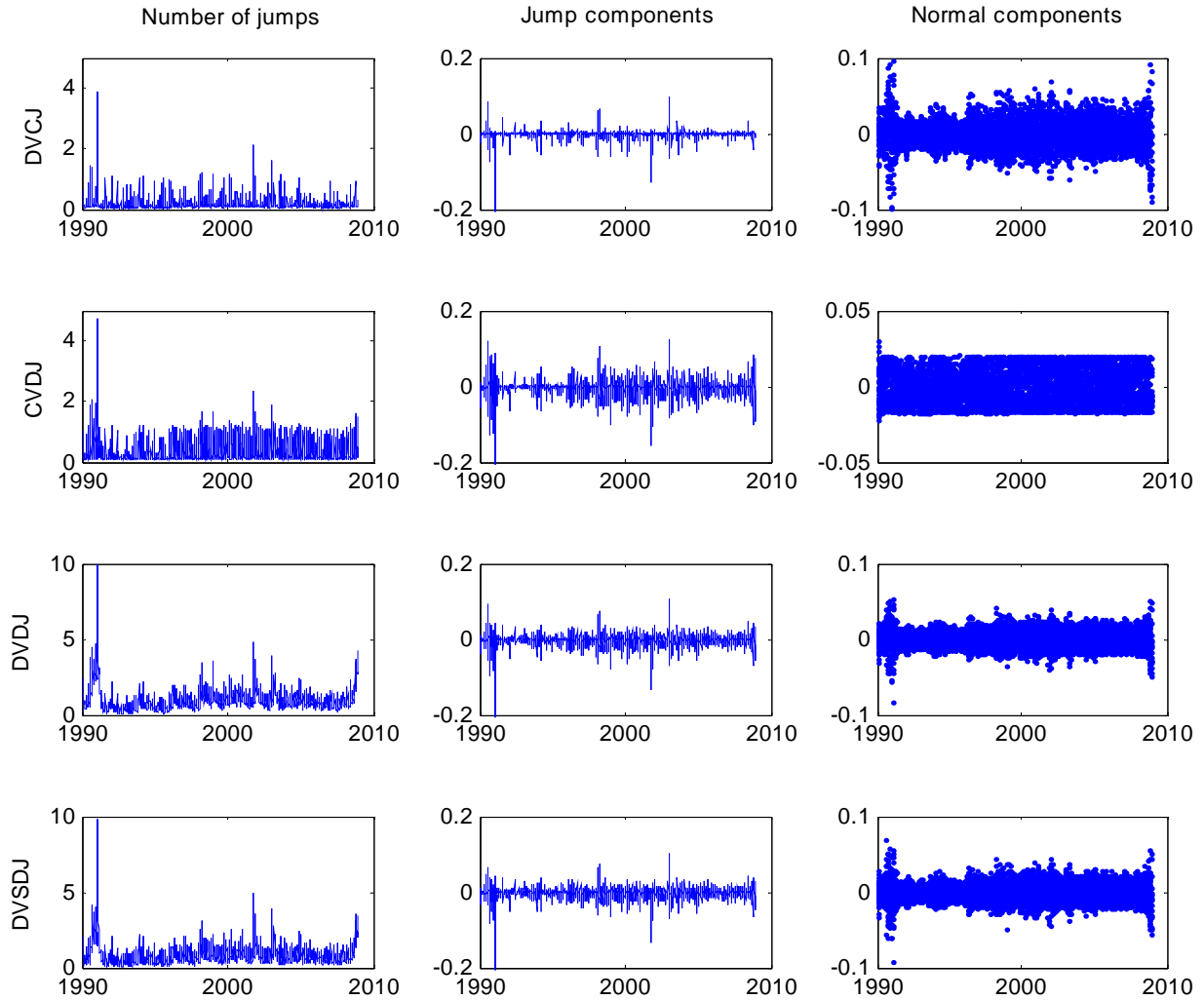


Figure 6. Decomposition of Daily Futures Returns Estimated Using Futures Contracts

We plot the filtered number of jumps, n_t , in the left column, the filtered jump component, y_t , in the middle column, and the filtered standardized normal component, z_t , in the right column for four jump models. Results are obtained using the analytical filter and the MLE estimates from Table 2.

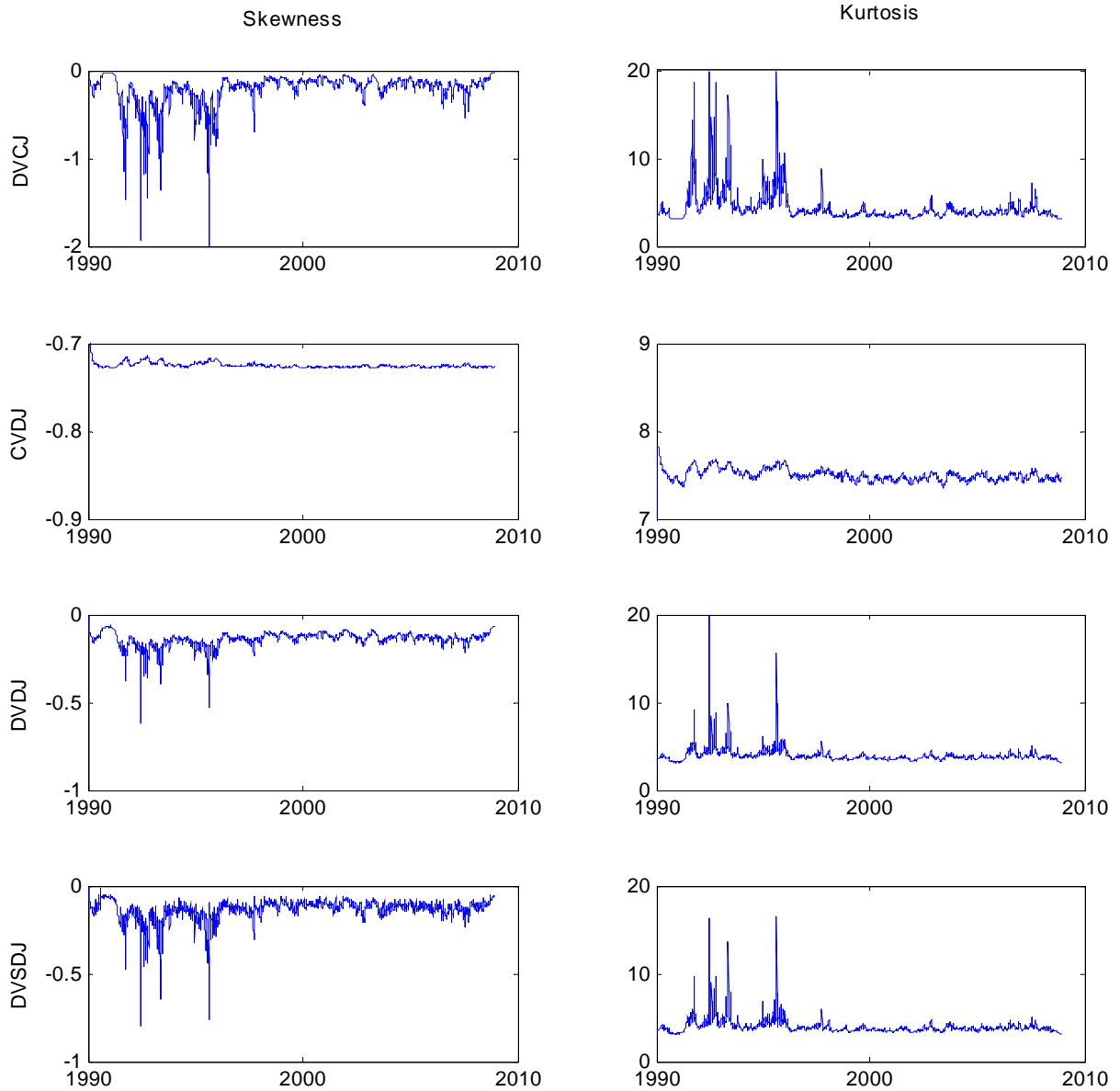


Figure 7. Conditional Skewness and Conditional Excess Kurtosis Estimated Using Futures Contracts

This figure plots daily conditional skewness in the left column and conditional excess kurtosis in the right column for four jump models.

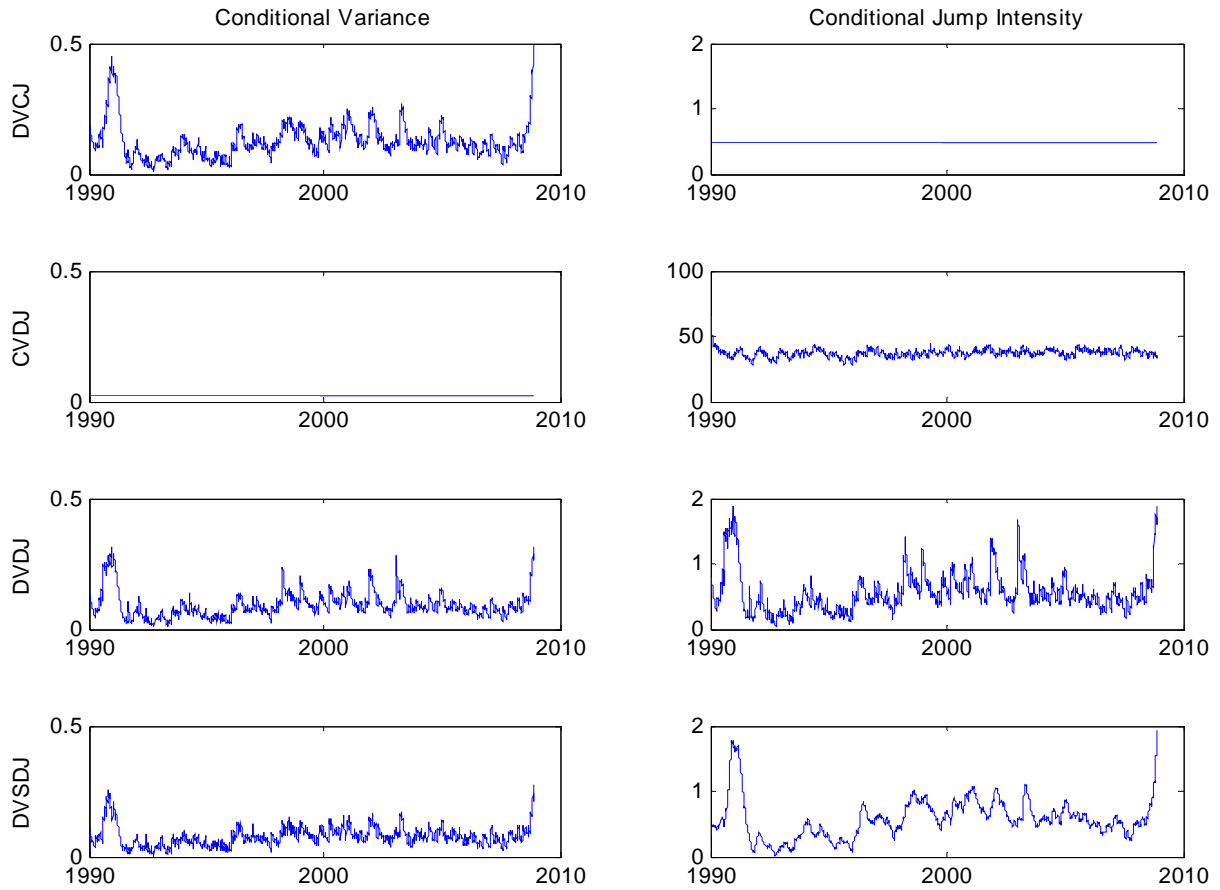


Figure 8. Conditional Variance and Jump Intensity Estimated Using Futures and Option Contracts.

We plot the annualized conditional variance, $h_{z,t+1}$, in the left column and the annualized conditional jump intensity, $h_{y,t+1}$, in the right column for four jump models.

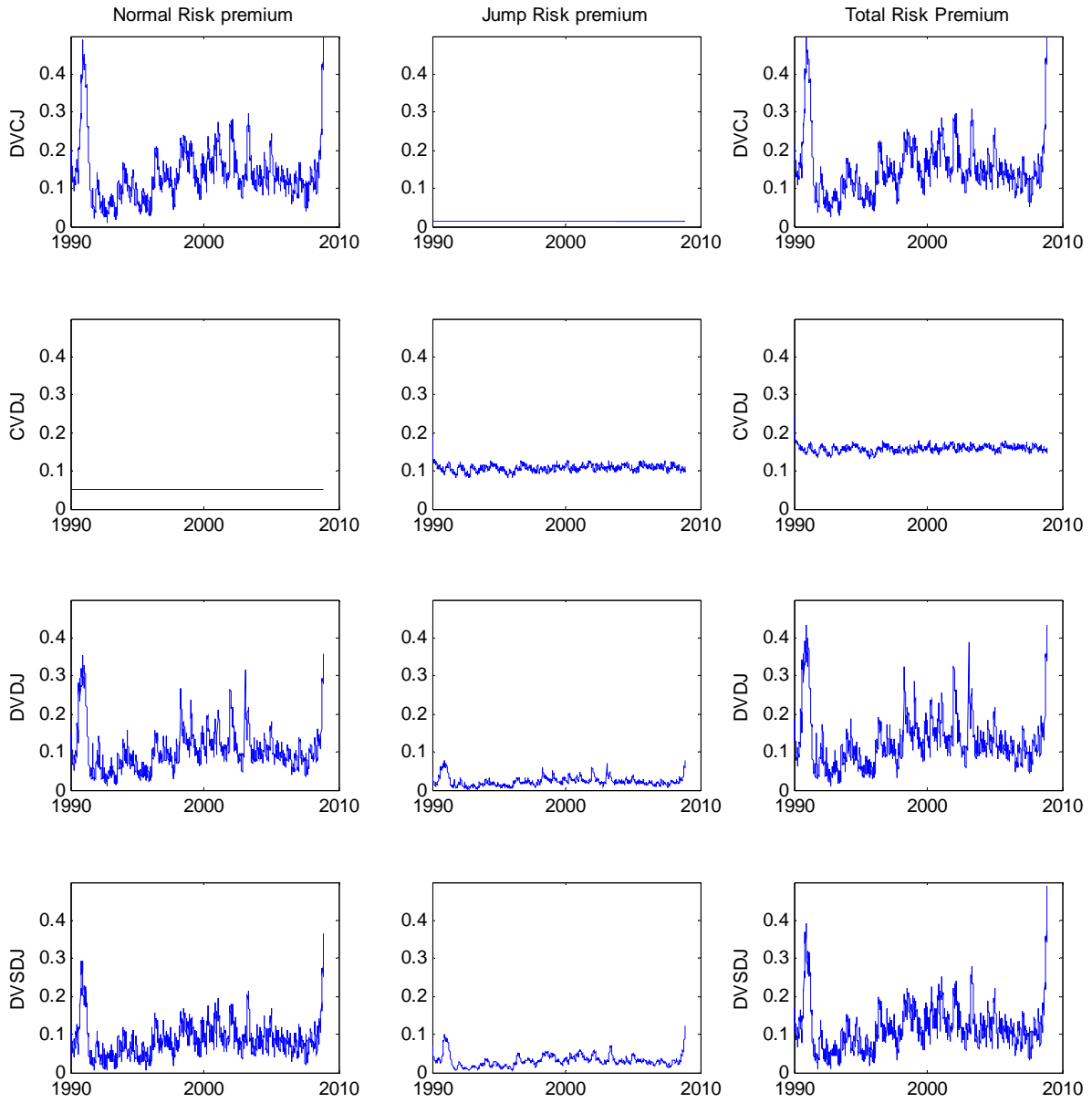


Figure 9. Risk Premiums Estimated Using Futures and Option Contracts

We plot the normal risk premium, $\gamma_{z,t} \equiv \lambda_z h_{z,t}$, in the left column, the jump risk premium, $\gamma_{y,t} \equiv \lambda_y h_{y,t}$, in the middle column, and the total risk premium, $\gamma_t \equiv \lambda_z h_z + \lambda_y h_y$, in the right column for four jump models.

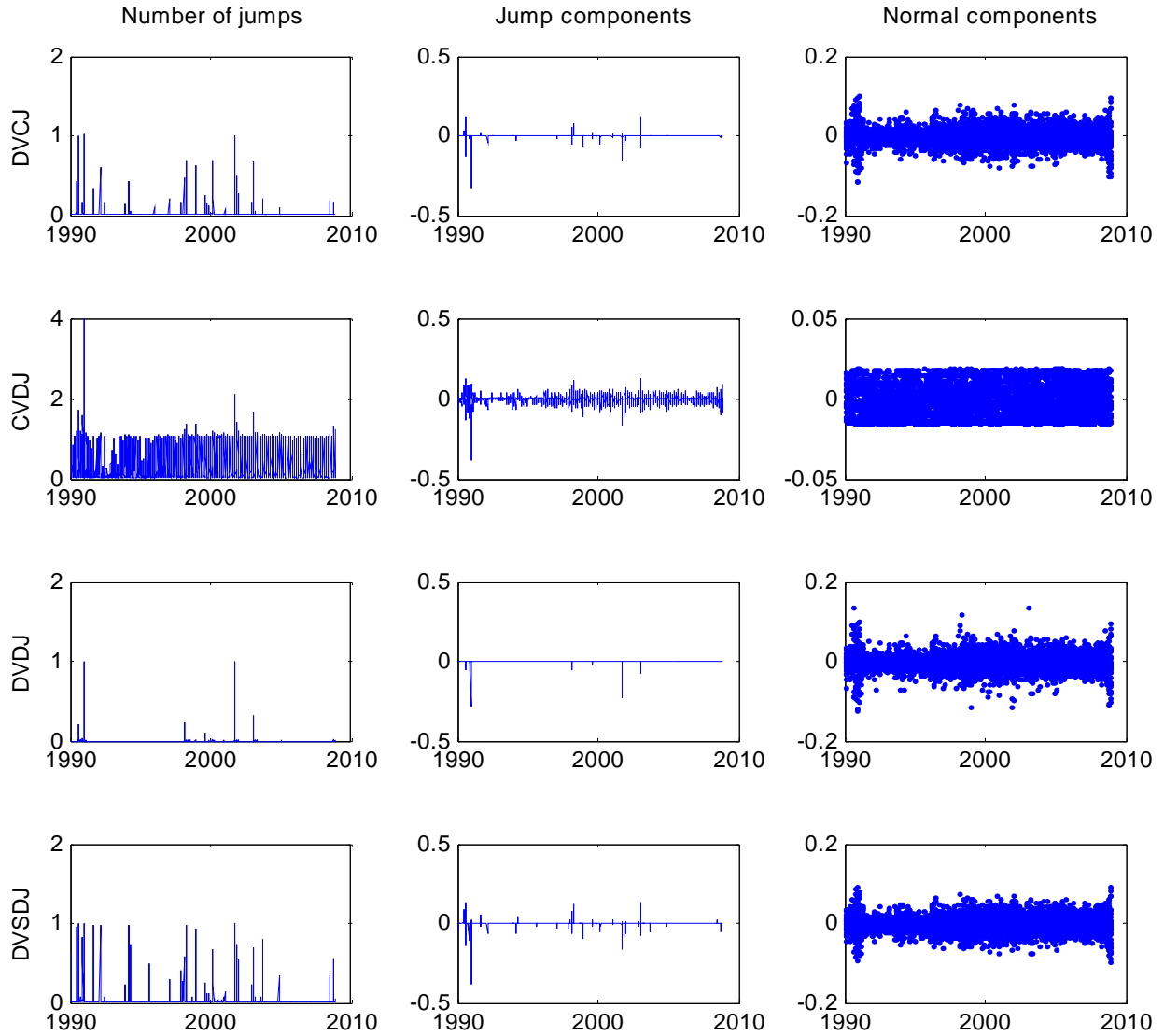


Figure 10. Decomposition of Daily Futures Returns estimated Using Futures and Option Contracts

We plot the filtered number of jumps, n_t , in the left column, the filtered jump component, y_t , in the middle column, and the filtered standardized normal component, z_t , in the right column for four jump models. Results are obtained using the analytical filter and the joint MLE estimates of futures and options from Table 5.

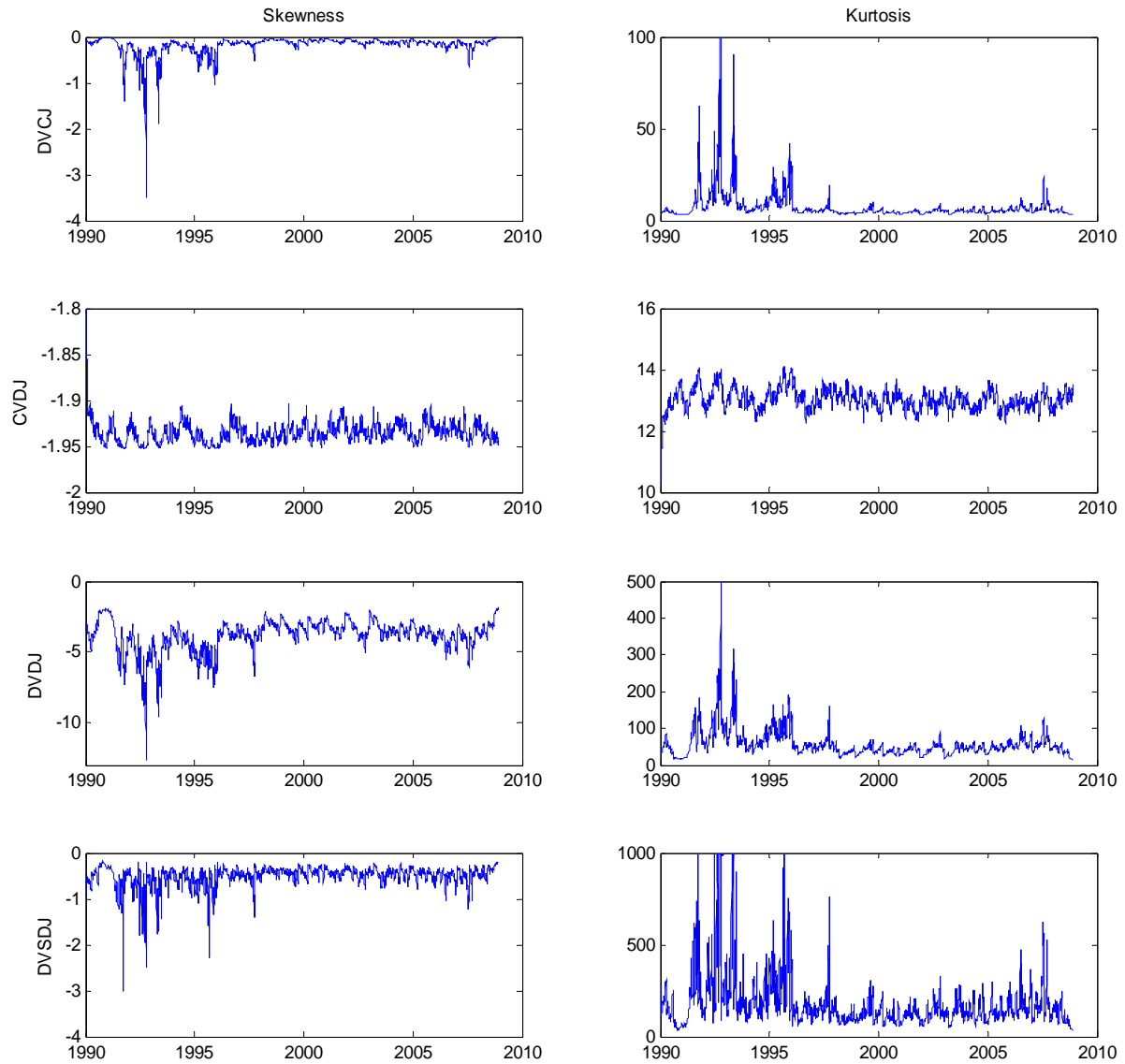


Figure 11. Conditional Skewness and Conditional Excess Kurtosis Estimated Using Futures and Option Contracts

We plot the daily conditional skewness in the left column and the conditional excess kurtosis in the right column for four jump models. The moments are estimated using joint MLE on futures and options data.

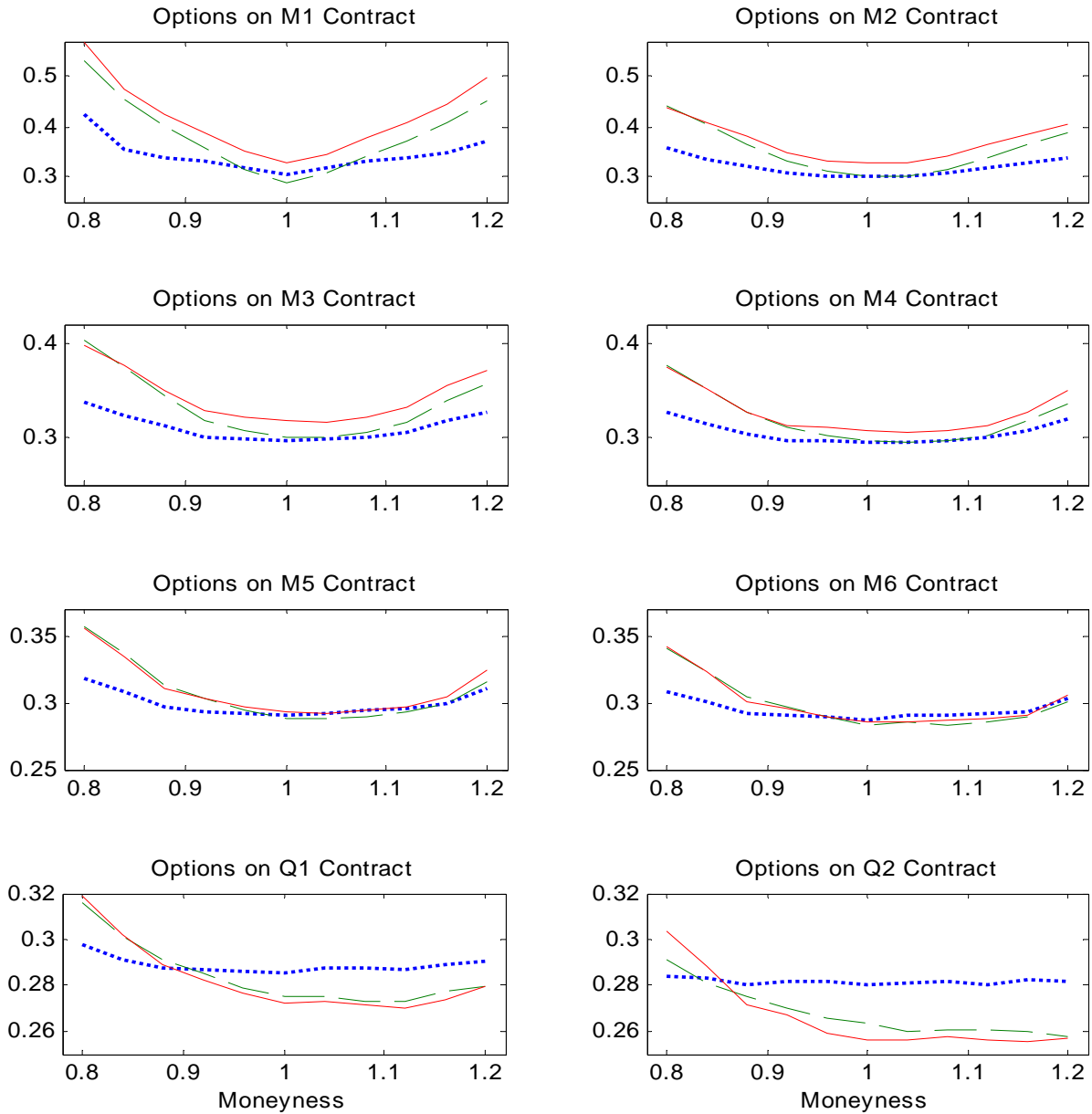


Figure 12. Average Implied Log-Normal Volatility “Smiles”

We plot the average implied volatility across moneyness. Moneyness is defined as the option strike divided by the price of the underlying futures contract. The red solid line “—” shows the average volatility smiles in the option data. The green dashed line “- - -” shows the average over time of the fitted smiles for the DVSDJ model. The blue dotted line “.....” shows the average over time of the fitted smile for the GARCH model. Model parameters are from Table 5. Averages are taken over a maximum of 4,753 daily observations from January 2, 1990 through December 3, 2008.